This article is a *Plant Cell* Advance Online Publication. The date of its first appearance online is the official date of publication. The article has been edited and the authors have corrected proofs, but minor changes could be made before the final version is published. Posting this version online reduces the time to publication by several weeks.

The *Trans*-Acting Short Interfering RNA3 Pathway and NO APICAL MERISTEM Antagonistically Regulate Leaf Margin Development and Lateral Organ Separation, as Revealed by Analysis of an *argonaute7/lobed leaflet1* Mutant in *Medicago truncatula*[W][OPEN]

Chuanen Zhou,[a] Lu Han,[a] Chunxiang Fu,[a] Jiangqi Wen,[b] Xiaofei Cheng,[b] Jin Nakashima,[b] Junying Ma,[b] Yuhong Tang,[b] Yang Tan,[a] Million Tadege,[c] Kirankumar S. Mysore,[b] Guangmin Xia,[d] and Zeng-Yu Wang[a,1]

[a] Forage Improvement Division, The Samuel Roberts Noble Foundation, Ardmore, Oklahoma 73401
[b] Plant Biology Division, The Samuel Roberts Noble Foundation, Ardmore, Oklahoma 73401
[c] Institute of Agricultural Biosciences, Oklahoma State University, Ardmore, Oklahoma 73401
[d] Key Laboratory of Plant Cell Engineering and Germplasm Innovation, Ministry of Education, School of Life Sciences, Shandong University, Jinan 250100, China

Leaf shape elaboration and organ separation are critical for plant morphogenesis. We characterized the developmental roles of *LOBED LEAFLET1* by analyzing a recessive mutant in the model legume *Medicago truncatula*. An ortholog of *Arabidopsis thaliana ARGONAUTE7* (*AGO7*), Mt-*AGO7*/*LOBED LEAFLET1,* is required for the biogenesis of a *trans*-acting short interfering RNA (ta-siRNA) to negatively regulate the expression of *AUXIN RESPONSE FACTORs* in *M. truncatula*. Loss of function in *AGO7* results in pleiotropic phenotypes in different organs. The prominent phenotype of the *ago7* mutant is lobed leaf margins and more widely spaced lateral organs, suggesting that the *trans*-acting siRNA3 (*TAS3*) pathway negatively regulates the formation of boundaries and the separation of lateral organs in *M. truncatula*. Genetic interaction analysis with the *smooth leaf margin1* (*slm1*) mutant revealed that leaf margin formation is cooperatively regulated by the auxin/SLM1 (ortholog of *Arabidopsis PIN-FORMED1*) module, which influences the initiation of leaf margin teeth, and the *TAS3* ta-siRNA pathway, which determines the degree of margin indentation. Further investigations showed that the *TAS3* ta-siRNA pathway and NO APICAL MERISTEM (ortholog of *Arabidopsis CUP-SHAPED COTYLEDON*) antagonistically regulate both leaf margin development and lateral organ separation, and the regulation is partially dependent on the auxin/SLM1 module.

INTRODUCTION

New organs are formed from meristems throughout the life cycle of a plant. Well-organized and regulated cell division and expansion are crucial for the patterning and elaboration of organ primordia, requiring a mechanism for reiterative specification of new boundaries (Aida and Tasaka, 2006; Berger et al., 2009). Auxin is one of the major plant hormones that has vast effects on plant developmental processes. The local auxin activity gradient generated by the auxin efflux regulator PIN-FORMED1 (PIN1) is one such mechanism that facilitates initiation of organs at the flanks of the shoot apical meristem (SAM). The polar localization of PIN1 in auxin-conducting cells determines the direction of auxin flow. Loss of function of PIN1 leads to defects in the separation of lateral organs (Vernoux et al., 2000; Reinhardt et al., 2003). Although the auxin accumulation pattern regulated by PIN1 is a prerequisite for the identification of boundaries during organ initiation, the creation of such boundaries also requires coordinated actions with other genes such as NAC-domain transcription factor genes (Aida and Tasaka, 2006; Blein et al., 2008; Rast and Simon, 2008; Berger et al., 2009). Leaf shape depends on the pattern of serrations and the degree of indentation of leaf margins. Previous studies have shown that two key processes are required for the development of leaf margins in *Arabidopsis thaliana*. The first process is the local auxin activity gradient generated by PIN1 (Hay et al., 2006). The formation of marginal serration tips is tightly correlated with auxin activity maxima, and the formation of lateral veins is defined by internalizing auxin through the center of the serrations. Perturbation of auxin transport by 1-*N*-naphthylphthalamic acid results in smooth leaf margins (DeMason and Chawla, 2004; Hay et al., 2006; Barkoulas et al., 2008; Zhou et al., 2011a). The second process is the repression of growth at the sinus by CUP-SHAPED COTYLEDON2 (CUC2). Two feedback loops involving PIN1 and CUC2 have been conceptualized for the formation of leaf serrations in *Arabidopsis* (Bilsborough et al., 2011).

Trans-acting short interfering RNAs (ta-siRNAs) are endogenous siRNAs that act in *trans* and direct the cleavage of complementary mRNA. The production of ta-siRNAs requires components from both microRNA and siRNA biogenesis pathways, including SUPPRESSOR OF GENE SILENCING3 (SGS3), RNA-DEPENDENT RNA

[1] Address correspondence to zywang@noble.org.
The author responsible for distribution of materials integral to the findings presented in this article in accordance with the policy described in the Instructions for Authors (www.plantcell.org) is: Zeng-Yu Wang (zywang@noble.org).
[W] Online version contains Web-only data.
[OPEN] Articles can be viewed online without a subscription.
www.plantcell.org/cgi/doi/10.1105/tpc.113.117788

POLYMERASE6 (RDR6), DICER-LIKE4 (DCL4), and ARGONAUTE7 (AGO7)/ZIPPY (ZIP) (Yoshikawa et al., 2005). In *Arabidopsis*, the transition from the juvenile to adult phases is suppressed by *trans*-acting siRNA3 (*TAS3*) in an AGO7-dependent manner through negative regulation of *AUXIN RESPONSE FACTOR3* (*ARF3/ ETTIN*) and *ARF4* mRNA expression (Adenot et al., 2006; Garcia et al., 2006; Hunter et al., 2006). The ARFs bind to the auxin-responsive element in the promoter of auxin-inducible genes to mediate auxin-dependent transcriptional regulation (Ulmasov et al., 1997). Among these ARFs, ARF3 and ARF4 function as repressors to mediate auxin response, and their activities are necessary for specifying abaxial leaf fate in *Arabidopsis* (Tiwari et al., 2001; Allen et al., 2005; Pekker et al., 2005). In addition, *ARF3* lacks the C-terminal dimerization domain that is required for heterodimerization with the auxin/indole-3-acetic acid protein. Therefore, it is unlikely that the activity of *ARF3* is regulated by auxin at the posttranscriptional level (Ulmasov et al., 1999; Guilfoyle and Hagen, 2001; Liscum and Reed, 2002).

The roles of ta-siRNAs in leaf patterning and leaf polarity vary substantially among species. The *Arabidopsis ago7* mutants display increased leaf length and downward-curled leaf margin; however, the mutants do not show obvious leaf polarity defects (Hunter et al., 2003, 2006; Fahlgren et al., 2006). Tomato (*Solanum lycopersicum*) *WIRY* genes are involved in ta-siRNA biogenesis, and the *wiry* mutants show shoestring leaves with defects in leaf blade expansion (Yifhar et al., 2012). In the legume species *Lotus japonicus*, mutations in *REDUCED LEAFLET1* (*REL1*) and *REDUCED LEAFLET3* (*REL3*), which respectively encode the orthologs of *Arabidopsis SGS3* and *AGO7,* result in abaxialized leaflets with decreased leaflet numbers (Yan et al., 2010). In monocots, more obvious developmental defects have been observed in ta-siRNA pathway–related mutants. Blocking of the *TAS3* ta-siRNA pathway in rice (*Oryza sativa*) leads to complete deletion or abnormal formation of the SAM (Liu et al., 2007; Nagasaki et al., 2007). In maize (*Zea mays*), the *leafbladeless1* mutant, which carries a mutation in *SGS3*, develops radially symmetric, thread-like leaves with partial or complete loss of adaxial cell identity (Timmermans et al., 1998; Juarez et al., 2004; Nogueira et al., 2007). However, the maize *ago7* mutant, *ragged seedling2*, maintains dorsiventral polarity of the leaf (Douglas et al., 2010).

A well-defined adaxial-abaxial domain in leaves is crucial for subsequent leaf expansion and leaf shape (Braybrook and Kuhlemeier, 2010; Wang et al., 2011). Independent studies have shown that the ta-siRNA pathway is broadly involved in the determination of dorsiventral polarity of leaves among species (Timmermans et al., 1998; Juarez et al., 2004; Liu et al., 2007; Yan et al., 2010). Therefore, the ta-siRNA pathway probably plays a key role in leaf morphogenesis. In the model legume *Medicago truncatula,* the orthologs of *Arabidopsis PIN1* and *CUC* have been identified and named *SMOOTH LEAF MARGIN1* (*SLM1*) and *NO APICAL MERISTEM* (*NAM*), respectively (Zhou et al., 2011a; Cheng et al., 2012). The *slm1* mutant exhibits a smooth leaf margin as a result of diffuse auxin distribution, suggesting the conserved roles of the auxin/SLM1 module in different plant species (DeMason and Chawla, 2004; Barkoulas et al., 2008; Koenig et al., 2009; Zhou et al., 2011a). In addition, the loss of function of SLM1 or NAM in *M. truncatula* leads to defects in the separation of lateral organs, indicating that both of them are positively correlated with the promotion of organ boundaries. However, thus far, it is not clear how plants prevent organs/tissues from overseparation during differential growth and morphogenesis. The regulator that plays negative roles in the formation of boundaries remains unclear. In this study, we analyzed the developmental roles of the *TAS3* ta-siRNA pathway in *M. truncatula* by characterizing a mutant with lobed leaf margins, *lobed leaflet1* (*lol1*). Molecular analyses show that *LOL1* is an ortholog of *Arabidopsis AGO7,* which is specifically required for the biogenesis of *TAS3* ta-siRNA. Loss of function of AGO7/LOL1 leads to pleiotropic defects in different plant organs as a result of the ectopic expression of target *ARF* genes. The prominent phenotype of the *ago7/lol1* mutants is a lobed leaf margin and more pronounced lateral organ separation, implying that the *TAS3* ta-siRNA pathway functions as a repressor during the formation of boundaries of organs/tissues in *M. truncatula*. Genetic interaction analyses with other mutants suggest that the *TAS3* ta-siRNA pathway and *NAM* antagonistically regulate leaf margin elaboration and lateral organ separation, and that such regulation is partially dependent on the auxin/SLM1 module.

RESULTS

LOL1 Regulates Leaf and Flower Development

Four mutant lines showing obvious changes in leaf margins were identified from screening ~10,000 *M. truncatula* mutants tagged by the transposable element of tobacco (*Nicotiana tabacum*) cell type1 (*Tnt1*). In contrast with the serrated leaf margin in the wild type (Figure 1A), all of these mutants displayed lobed leaf margins (Figure 1B). The mutants were thus named *lobed leaflet1* (*lol1-1* to *lol1-4*).

Although *M. truncatula* is a compound leaf species, its leaf development is heteroblastic. The first true leaf, also called the juvenile leaf, has simple leaf morphology (Figures 1C and 1D). All adult leaves that subsequently develop are in trifoliate form (Figures 1A and 1C). In the juvenile leaf, ~43% of the mutants showed one or two extra lateral leaflets (Figures 1E to 1G). In the adult phase, *lol1-1* exhibited lobed and elongated adult leaves (Figure 1B; see Supplemental Table 1 online). These observations suggest that loss of function of LOL1 has different effects on leaf development at the juvenile and adult stages. Anatomical analysis revealed that the phloem was enlarged on the abaxial side of leaves and the palisade mesophyll cells became smaller in *lol1-1* compared with those of the wild type (Figures 1H and 1I). Cross sections of petioles in the wild type showed that three vascular bundles were arranged in a polar fashion, and two of them were located on the adaxial side of the petiole (Figure 1J). By contrast, the number of vascular bundles on the adaxial side of the petiole was decreased in *lol1-1* (Figure 1K). In addition, the shape of cross sections of petioles in *lol1-1* was changed to nearly round. These observations indicate that the polarity of lateral organs is altered and that these organs are partially abaxialized in *lol1-1*.

Flowers developed in *lol1-1* were abnormal and the plants were infertile. The *M. truncatula* flower contains three types of petals. The largest petal (vexillum) is located at the adaxial position of the flower. Two lateral petals (alae) and two fused short petals (keel) are fused at the basal region and are situated at the abaxial side of the flower (Figures 2A to 2D) (Benlloch et al., 2003). More widely

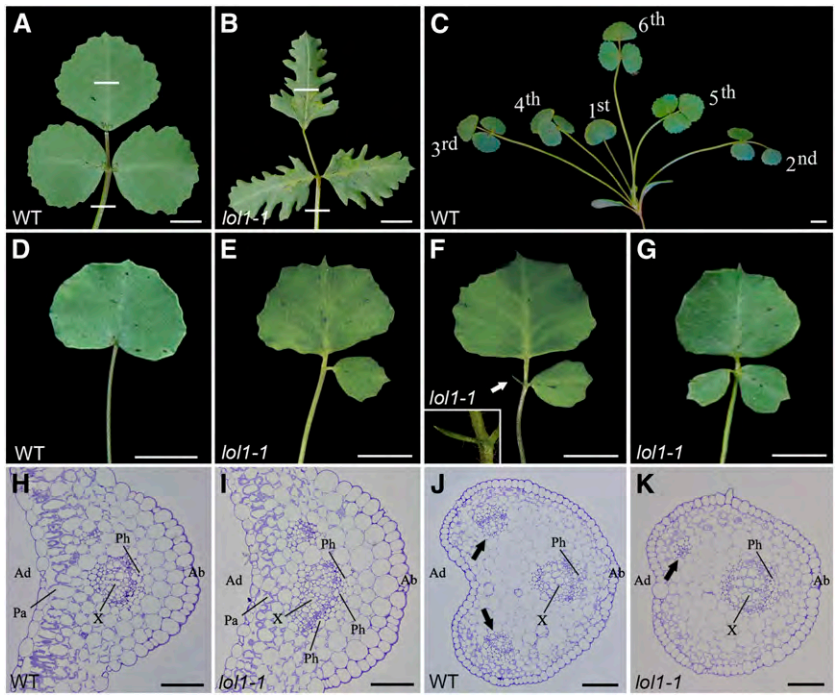

Figure 1. *lol1-1/ago7-1* Mutant of *M. truncatula* Shows Defects in Leaf Development.

(A) Adult leaf of the wild type.
(B) Adult leaf of *lol1-1/ago7-1* mutant.
(C) Four-week-old plant of the wild type. One juvenile leaf (first) and five adult leaves (second to sixth) are marked based on the order of leaf initiation.
(D) to **(G)** Juvenile leaf of the wild type **(D)** and *lol1-1/ago7-1* (**[E]** to **[G]**). The juvenile leaf of *lol1-1/ago7-1* exhibits additional leaflets. The inset in **(F)** shows a close view of the rod-shaped leaflet indicated by an arrow.
(H) to **(K)** Transverse sections of terminal leaflets in the wild type **(H)** and *lol1-1/ago7-1* **(I)**, and petioles in the wild type **(J)** and *lol1-1/ago7-1* **(K)**. The sectioning regions are shown in **(A)** and **(B)** by white lines, respectively. Arrows point to the vascular bundles on the adaxial side.
Ab, abaxial side; Ad, adaxial side; Pa, palisade mesophyll cell; Ph, phloem; WT, wild type; X, xylem.
Bar in **(A)** to **(G)** = 5 mm; bar in **(H)** to **(K)** = 200 μm.

spaced keel and alae were observed in *lol1-1*, suggesting that LOL1 affects the boundary formation of floral organs (Figures 2E to 2H). Furthermore, the lesion in LOL1 resulted in defects in the central carpel, anther dehiscence, and pollen viability (Figures 2I to 2P). As a result, mature plants of all four alleles of *LOL1* failed to develop seedpods.

LOL1 Encodes an ARGONAUTE Protein

Flanking sequences of *Tnt1* retrotransposon in *lol1-1* were recovered by thermal asymmetric interlaced PCR, and one of the sequences was confirmed to be associated with the mutation. A genomic sequence of 4088 nucleotides was obtained by blasting this flanking sequence against the *M. truncatula* genomic sequences. The full-length coding sequence (CDS) of *LOL1* contains 3057 nucleotides (Figure 3A). PCR amplification of the *LOL1* genomic sequence from the four alleles and the wild type revealed that all mutants carried a single 5.3-kb insertion (Figure 3B). Further analysis showed that a *Tnt1* retrotransposon was inserted in exons of *LOL1* in *lol1-1*, *lol1-2*, and *lol1-3*. However, *lol1-4* carried a native retrotransposon, *Medicago RetroElement1* (Rakocevic et al., 2009) (Figure 3A). The expression of *LOL1* was interrupted in all four *lol1* alleles (Figure 3C). Furthermore, the defects in *lol1-1* were fully rescued after transforming the *LOL1* CDS driven by the native or the cauliflower mosaic virus 35S promoter into homozygous mutant plants (see Supplemental Figure 1 and Supplemental Table 1 online). No obvious phenotypic changes were observed in *LOL1*-overexpressing lines in the wild type (see Supplemental Figure 1 online). Bioinformatic analysis showed that LOL1 belongs to the ARGONAUTE protein family and is the putative ortholog of the *Arabidopsis* AGO7 in *M. truncatula* (see Supplemental Figure 2 and Supplemental Data Set 1 online). To allow consistent nomenclature, we renamed LOL1 as AGO7.

RT-PCR analysis revealed that *AGO7* was expressed in almost all tissues. The expression level of *AGO7* was relatively high in flowers, stems, and leaves, and relatively low in cotyledons, pods, and roots (Figure 3D). RNA in situ hybridization was conducted to further examine the spatial expression patterns of *AGO7*. At the vegetative stage, preferential expression of *AGO7* was observed on the adaxial side of the emerging leaf primordia and developing leaflets but not in the SAM (Figures 3E to 3G). In the reproductive stage, higher levels of *AGO7* expression were detected in the floral meristem and developing floral organs such as petals and ovules (Figures 3H to 3J). These data indicate that *AGO7* plays a role in

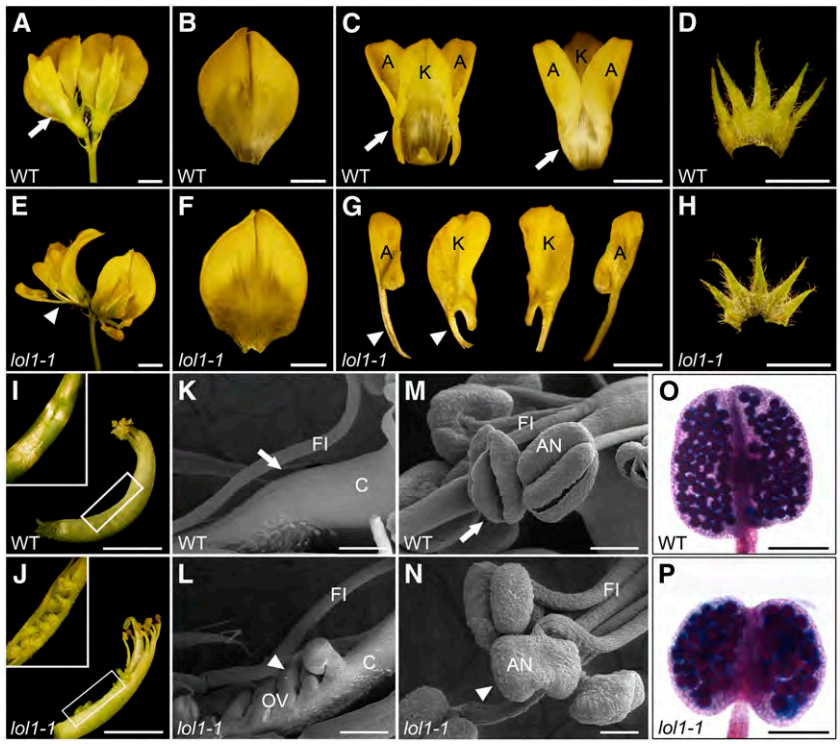

Figure 2. *lol1-1/ago7-1* Mutant of *M. truncatula* Shows Defects in Flower Development.

(A) Flower phenotype in the wild type. Arrow points to the bottom of fused alae and keel.
(B) to **(D)** Dissected floral organs of the wild type. The top view of vexillum **(B)**, the top view (left) and bottom view (right) of fused alae and keel **(C)**, and the top view of a dissected sepal **(D)**. Arrows point to the bottom of fused alae and keel.
(E) Flower phenotype in the *lol1-1/ago7-1*. Arrowhead points to the overseparated alae and keel.
(F) to **(H)** Dissected floral organs of the *lol1-1/ago7-1*. The top view of vexillum **(F)**, the separated alae and keel **(G)**, and the top view of a sepal **(H)**. Arrowheads point to the basal regions of overseparated alae and keel.
(I) and **(J)** The side view of the central carpel in the wild type **(I)** and *lol1-1/ago7-1* **(J)**. The insets in **(I)** and **(J)** show the top view of central carpels.
(K) and **(L)** Scanning electron microscopy analysis of the central carpel in the wild type **(K)** and *lol1-1/ago7-1* **(L)**. Arrow in **(K)** points to the closed central carpel. Arrowhead in **(L)** points to the opened central carpel and exposed ovules.
(M) and **(N)** Scanning electron microscopy analysis of anthers in the wild type **(M)** and *lol1-1/ago7-1* **(N)**. Arrow in **(M)** points to the dehiscing anther. Arrowhead in **(N)** shows defect in anther dehiscence in *lol1-1/ago7-1*.
(O) and **(P)** Pollen staining in the wild type **(O)** and *lol1-1/ago7-1* **(P)**. The size of pollen and anther sacs was uneven and pollen was partially viable in *lol1-1/ago7-1*.
A, alae; AN, anther; C, carpel; FI, filament; K, keel; OV, ovule; WT, wild type.
Bar in **(A)** to **(J)** = 2 mm**;** bar in **(K)** to **(P)** = 200 μm.

plant development in both the vegetative and reproductive stages. In addition, the asymmetric expression pattern in leaf primordia implies that *AGO7* is probably involved in the establishment of adaxial/abaxial leaf polarity, as also evidenced by the defects in dorsiventral polarity in the *ago7-1* mutant (Figures 1H to 1K).

AGO7 Functions in the *TAS3* ta-siRNA Pathway in *M. truncatula*

It has been shown that AGO7 is specifically required for *TAS3* ta-siRNA (Montgomery et al., 2008). To determine whether *AGO7* plays a similar role in the *TAS3* ta-siRNA pathway in *M. truncatula*, a putative *TAS3* ta-siRNA gene (AC186679.3) was obtained by conducting a BLAST database search. Two 21-nucleotide–long *TAS3* ta-siRNAs were identified based on the sequences of the *TAS3* ta-siRNA precursor and miR390 in *M. truncatula* (Figure 4A). The *TAS3* ta-siRNAs showed high similarity with those in other species (Figure 4B). Furthermore, the transcript levels of *TAS3 5′D7 (+)* and *TAS3 5′D8 (+)* were dramatically reduced, whereas *miR390* was accumulated in *ago7-1*, indicating that the *AGO7* gene is required for the biogenesis of *TAS3* ta-siRNA in *M. truncatula* (Figure 4C).

Microarray analysis was performed to determine the target genes of *TAS3* ta-siRNAs in *M. truncatula* (see Supplemental Data Sets 2 and 3 online). The expression levels of three *M. truncatula ARF* genes were upregulated dramatically in *ago7-1*, suggesting that they are the putative targets of *TAS3* ta-siRNAs. Phylogenetic analysis revealed that one ARF (AC158497_40.1, designated ARF3) is the putative ortholog of *Arabidopsis* ARF3. The other two (AC152176_2.1 and AC150891_17.1, designated

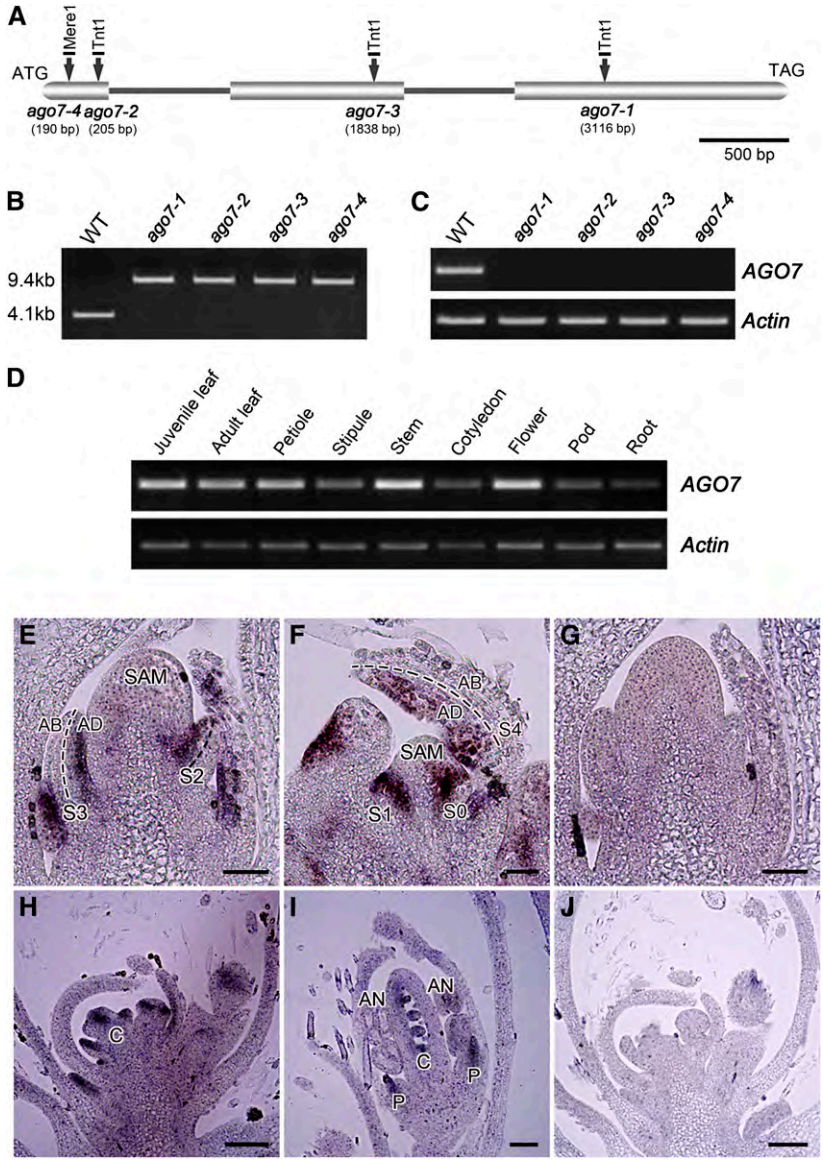

Figure 3. Molecular Cloning and Expression Pattern of *AGO7* in *M. truncatula*.

(A) Schematic representation of the gene structure of *AGO7*. Three exons (block) and two introns (line) are shown. Numbers indicate nucleotide positions of the site of mutations.
(B) PCR amplification of *AGO7* from the wild type and *ago7* mutants. A single insertion (~5.3 kb) was detected in each mutant line.
(C) RT-PCR analysis of *AGO7* transcripts in the wild type and *ago7* mutants. *Actin* was used as the loading control. Three technical replicates were performed.
(D) RT-PCR analysis of *AGO7* expression in different plant organs. *Actin* was used as the loading control. Three technical replicates were performed.
(E) to **(J)** In situ hybridization analysis of *AGO7* mRNA in vegetative and reproductive apices of the wild type. Bar = 50 μm in **(E)** to **(J)**.
(E) to **(G)** Longitudinal sections of the SAM at stages 3 and 4 (**[E]** and **[F]**, respectively). The sense probe was hybridized and used as the control **(G)**.
(H) to **(J)** Longitudinal sections of the floral apical meristem at stages 5 and 7 (**[H]** and **[I]**). The sense probe was hybridized and used as the control **(J)**.
AB, abaxial; AD, adaxial; AN, anther; C, carpel; P, petal; S, stage; WT, wild type.

ARF4a and ARF4b, respectively) are evolutionarily closer to *Arabidopsis* ARF4 and show high identity (71%) with each other. Therefore, they are probably the duplicated ARF4 orthologs in *M. truncatula* (see Supplemental Figure 3 and Supplemental Data Set 4 online). *ARF3* and *ARF4a/b* are highly expressed in multiple organs, implying that they play broad roles during plant development (see Supplemental Figure 4 online). Further analysis showed that all three *ARF* genes contained two recognition sites (A and B) that are complementary to the *TAS3* ta-siRNAs (Figure 4D). Quantitative RT-PCR (qRT-PCR) analysis showed

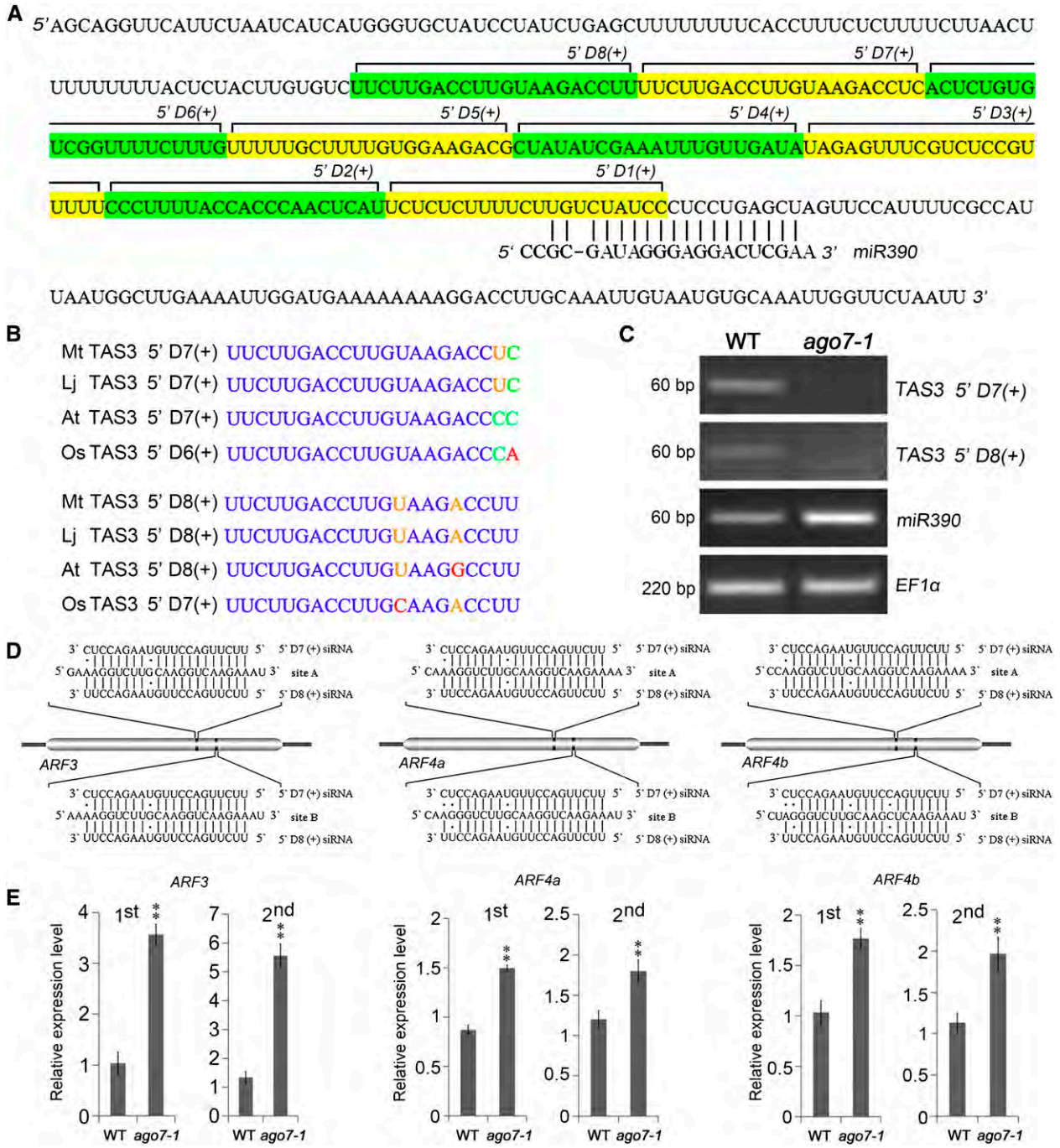

Figure 4. Characterization of Putative *TAS3* ta-siRNA and Target Genes in *M. truncatula*.

(A) A diagram represents the biogenesis of predicted *TAS3* ta-siRNAs from *TAS3* transcript directed by miR390. Putative ta-siRNAs are shown alternately in yellow and green.

(B) Alignment of *TAS3* ta-siRNAs among Mt (*M. truncatula*), Lj (*L. japonicus*), At (*Arabidopsis*), and Os (rice).

(C) RT-PCR analyses of *TAS3 5′D7(+)*, *TAS3 5′D8(+)*, and *miR390* in the wild type (WT) and *ago7-1*. *EF1*α was used as a control. Three technical replicates were performed.

(D) Diagram represents *TAS3* ta-siRNA and the coding sequence of three putative target *ARF* genes.

(E) Relative expression level of three *ARF* genes in the juvenile leaf (first foliage leaf) and second foliage leaf of the wild type and *ago7-1*. Values are the mean and SD of three biological replicates. *P < 0.05; **P < 0.01.

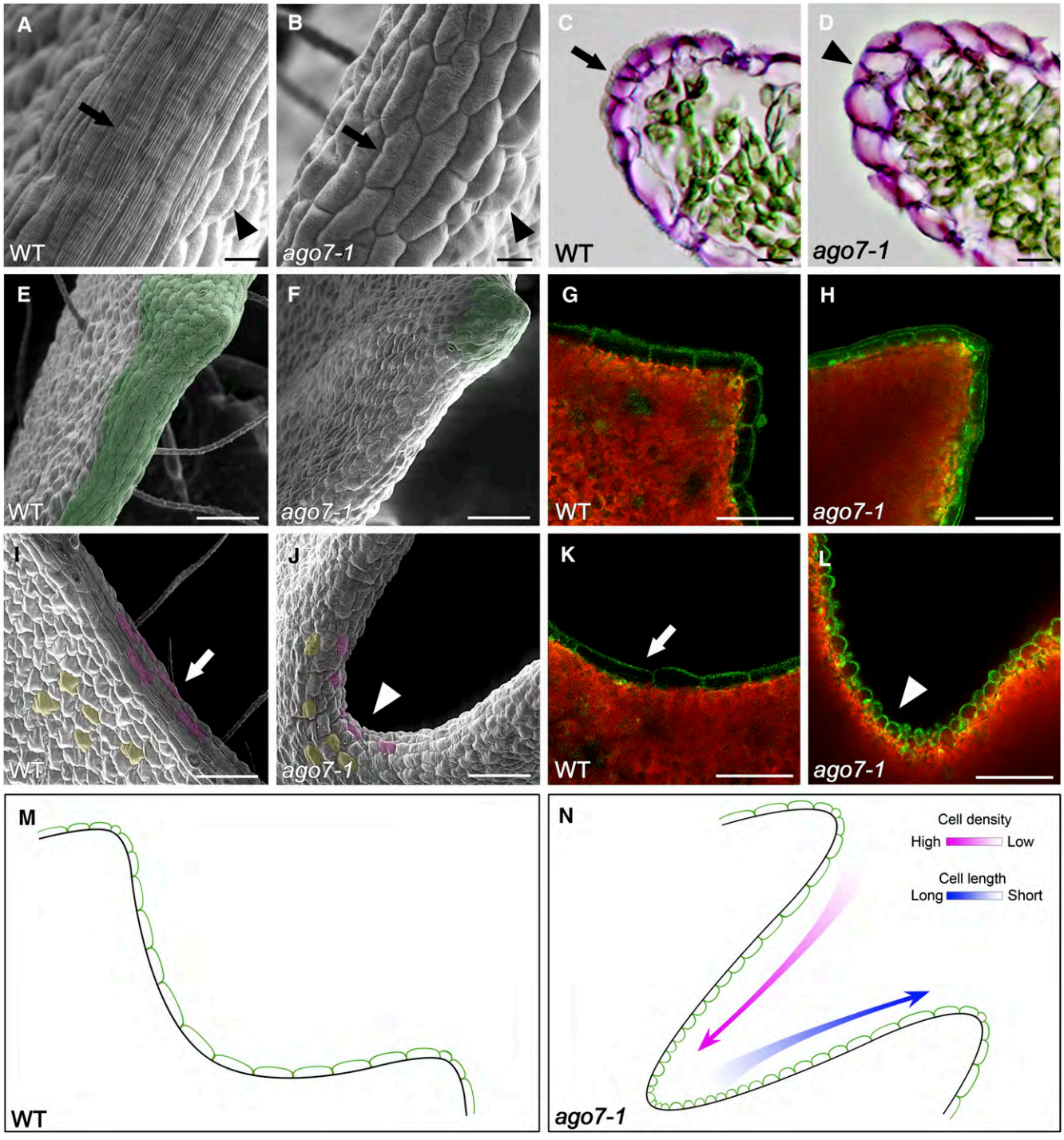

Figure 5. Involvement of AGO7 in Leaf Margin Development in *M. truncatula*.

(A) and **(B)** Observation of margin cells in the wild type (WT) **(A)** and *ago7-1* **(B)** by scanning electron microscopy. Arrows point to the margin cells. Arrowheads point to the epidermal cells.

(C) and **(D)** Transverse sections of leaf margin in the wild type **(C)** and *ago7-1* **(D)**. Arrow points to the ridge-like structure on the surface of margin cells in the wild type. Arrowhead points to the smooth surface of margin cells in *ago7-1*.

(E) to **(H)** Observation of margin cells at the teeth tips in the wild type **([E]** and **[G])** and *ago7-1* **([F]** and **[H])**. Margin cells harboring the auxin response marker DR5 (*DR5rev:GFP*) were observed by scanning electron microscopy **([E]** and **[F])** and confocal microscopy **([G]** and **[H])**. Cells with the ridge-like structure on the surface are marked in green in **(E)** and **(F)**.

that expression levels of the three *ARF* genes were significantly upregulated in *ago7-1* leaves at different stages (Figure 4E; see Supplemental Figure 5 online). These results suggest that *ARF3* and *ARF4a/b* are the putative targets of the *TAS3* ta-siRNA pathway.

The *TAS3* ta-siRNA Pathway Regulates Leaf Margin Development in *M. truncatula*

One prominent phenotype of *ago7-1* is the conversion of the serrated leaf margin to the lobed leaf margin. In the wild type, leaf margin tips started to initiate along the leaf margin after the formation of leaflet primordia (see Supplemental Figures 6A to 6H online). Compared with the wild type, *ago7-1* exhibited more pronounced leaf serration and sinuses (see Supplemental Figures 6I to 6P online). In addition, a ridge-like structure was observed on the surface of leaf margin cells in the wild type. By contrast, *ago7-1* exhibited a smooth surface of leaf margin cells that was similar to that of epidermal cells (Figures 5A to 5F). These observations indicate that leaf margin cells in *ago7-1* probably lost the determination of cell fate.

To monitor auxin responsiveness in leaf margin cells, the *DR5rev:green fluorescent protein (GFP)* reporter was transformed into wild-type and *ago7-1* plants. By examining the GFP expression signal, a higher level of auxin responsiveness was observed in the margin cells of *ago7-1* compared with those in the wild type (Figures 5G and 5H). GFP signal also offers a convenient way of visualizing cell size. At the tooth tip, the size of margin cells in *ago7-1* was similar to that of the wild type (Figures 5G and 5H). In the sinus, the margin cells (purple color) of the wild type were morphologically elongated compared with epidermal cells (yellow color) (Figure 5I). However, the size of margin cells in the sinus of *ago7-1* was similar to that of epidermal cells (Figure 5J). Furthermore, large numbers of small, nonelongated margin cells were observed in the sinus of *ago7-1* compared with the wild type (Figures 5K and 5L). Taken together, these data demonstrate that the lobed leaf of *ago7-1* is caused by increased cell proliferation activity and repressed elongation of margin cells in the sinus of the leaf margin (Figures 5M and 5N).

Lobed Leaf Margin in *ago7-1* Is Caused by the Ectopic Expression of *ARF3*

In fully expanded leaves, the expression of *ARF3* was increased by ~13-fold in *ago7-1,* whereas *ARF4a* and *ARF4b* were upregulated by approximately twofold compared with the wild type (see Supplemental Figure 5 online), implying that the ectopic expression of *ARF3* is the primary cause of the *ago7-1* phenotype. Three experiments were performed to verify this hypothesis. First, the expression pattern of *ARF3* was compared between the wild type and *ago7-1* by in situ hybridization. In the wild type, a weak expression of *ARF3* was detected in SAM. In the leaf primordia at the plastochron 2 (P2) stage, abaxial expression of *ARF3* was displayed (Figure 6A). By contrast, *ARF3* was highly expressed over a much broader region throughout the leaf primordia in *ago7-1*, suggesting that *ARF3* expression is repressed by the *TAS3* ta-siRNA pathway during leaf primordia development (Figure 6A). Second, *ARF3* knockdown ($ARF3_{RNAi}$) plants were generated using RNA interference in the *ago7-1* background. The expression level of *ARF3* was dramatically reduced in *ago7-1* transgenic plants, and the lobed leaf margin was completely recovered (Figures 6B to 6G). The transcript levels of *ARF4a* and *ARF4b* in the $ARF3_{RNAi}$ *ago7-1* plants were similar to that in *ago7-1* (see Supplemental Figure 7 online). These data suggest that the lobed leaf margin in *ago7-1* was specifically caused by the misexpression of *ARF3*. Third, to further confirm the above observations, the original *ARF3* cDNA (*OX-ARF3*) and a mutated *ARF3* cDNA carrying two altered *ta-siARF* target sites (*OX-ARF3mut*; Figure 6B) were introduced into wild-type plants under the regulation of the cauliflower mosaic virus 35S promoter, respectively. The expression level of *ARF3* was significantly upregulated in both the *OX-ARF3* and the *OX-ARF3mut* transgenic plants (Figure 6C). *OX-ARF3* plants exhibited downward-curled leaves and showed more serrations along the leaf margin (Figures 6H to 6J). By contrast, *OX-ARF3mut* transgenic plants displayed obvious lobed leaf margin, mimicking the *ago7-1* phenotype (Figures 6K to 6M). Taken together, these observations demonstrate that the lobed leaf margin in *ago7-1* is caused by the ectopic expression of *ARF3*.

ARF3 Expression Pattern and Auxin Responsiveness Is Altered in the Leaf Margin of *ago7-1*

To further evaluate the expression pattern of *ARF3* in the leaf, the transcript level of *ARF3* was examined in different regions of leaves in the wild type and *ago7-1* by dissecting the leaves into three regions (Figure 6N). In wild-type leaves, the expression of *ARF3* was similar in the middle and marginal (outer) regions, and the expression in both of these regions was lower than that of the inner region of the leaf. In *ago7-1,* a significantly higher level of *ARF3* expression was detected in the marginal region than in the middle region (Figure 6N). Characterization of transgenic plants carrying *DR5:GUS* and *DR5rev:GFP* constructs revealed that β-glucuronidase (GUS) activity or GFP signal was slightly increased in lateral leaf primordia and highly increased in floral organs and leaf margins, especially in the leaf teeth of *ago7-1* (Figure 6O; see Supplemental Figure 8 online). The results indicate the auxin responsiveness was changed. To test whether the transcription of *ARF3* depends on auxin, the expression level of

Figure 5. (continued).

(I) to **(L)** Observation of margin cells in the leaf sinus in the wild type **([I]** and **[K])** and *ago7-1* (**[J] and [L]**). The margin cells are marked in purple and epidermal cells are marked in yellow in **(I)** and **(J)**. Arrows point to the elongated margin cells in the wild type. Arrowheads point to the small and unelongated margin cells in *ago7-1*.

(M) and **(N)** A schematic illustration of the developmental difference of leaf margin cells in the wild type **(M)** and *ago7-1* **(N)**.

Bar in **(A)** to **(D)** = 20 μm; bar in **(E)** to **(L)** = 100 μm.

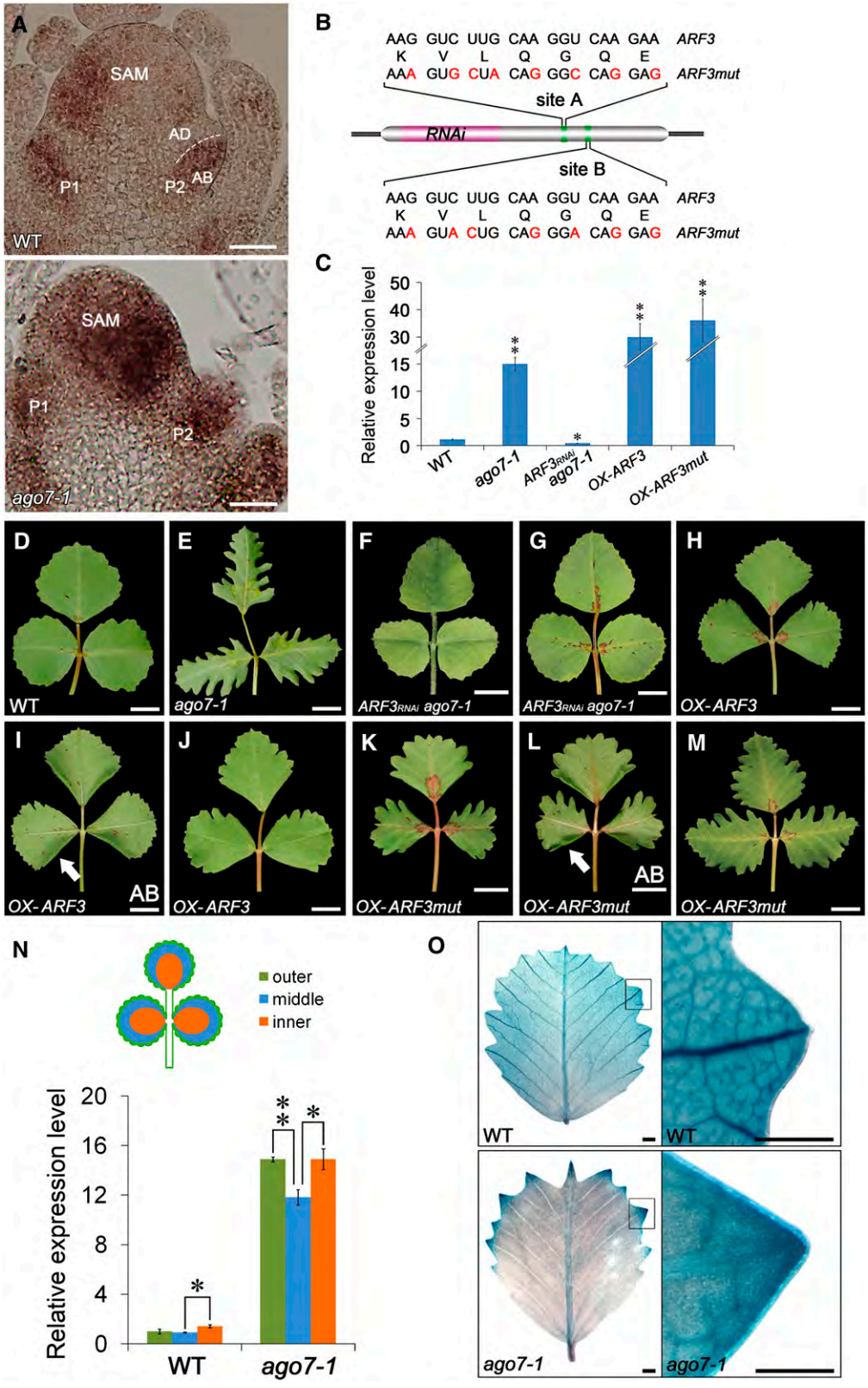

Figure 6. *ARF3* Expression Pattern and Auxin Distribution Is Altered in *ago7-1*.

ARF3 was measured in leaves treated with indole-3-acetic acid. No change in *ARF3* expression was observed in response to exogenous application of auxin (see Supplemental Figure 9 online). Therefore, the alteration of the *ARF3* expression pattern in leaf margins was not caused directly by altered auxin responsiveness in *ago7-1*.

Formation of Lobed Leaf Margin in *ago7-1* Is Partially Dependent on the Auxin/SLM1 Module

A previous study showed that SLM1 regulates leaf development by generating local auxin activity gradients (Zhou et al., 2011a). Compared with the wild type, the expression levels of *SLM1* were reduced in both leaf buds (Figure 7A) and fully expanded leaves in *ago7-1* (Figures 7B and 7C). The results were further confirmed by assaying the expression of the *SLM1* promoter–GUS reporter in wild-type and *ago7-1* backgrounds (Figures 7D to 7G).

The role of SLM1 in the formation of lobed leaf margin in *ago7-1* was further examined by generating a double mutant between *slm1-1* and *ago7-1* (Figures 7H to 7K). Both the *slm1-1* single mutant and *slm1-1 ago7-1* double mutant could produce a few leaf teeth at the early stage, and the numbers of teeth are similar between them (see Supplemental Figure 10 online). The leaf margin in *slm1-1* eventually became smooth because of a disruption of auxin distribution (Figure 7J) (Zhou et al., 2011a). However, a few serrations were formed in the *slm1-1 ago7-1* double mutant (Figure 7K). To further compare the leaf shape among the wild type and mutants, the terminal leaflets were outlined and overlapped with different colors (Figure 7L). The length and width of the terminal leaflet in the double mutant were intermediate between those of the two single mutants. Moreover, the contours of the terminal leaflet in the double mutant were similar to that of the wild type and distinct from those in single mutants. These observations suggest that the lobed leaf in *ago7* is partially dependent on the auxin/SLM1 module.

The *TAS3* ta-siRNA Pathway and NAM Antagonistically Regulate Leaf Margin Serration Development and Lateral Organ Separation

A recent study showed that NAM, a putative *M. truncatula* ortholog of NAM/CUC, is involved in the development of organ boundaries in *M. truncatula* (Cheng et al., 2012). The strong allele, *nam-1*, cannot maintain the SAM, resulting in a seedling-lethal phenotype. *nam-2* is a weak allele that can produce leaves and shoots showing fused leaflets and wild-type–like leaf margins (Cheng et al., 2012). Previous studies showed that NAM/CUC plays conserved roles among species in the regulation of both leaf margin development and lateral organ separation among species (Blein et al., 2008). Therefore, we hypothesized that NAM is also involved in the elaboration of the leaf margin in *M. truncatula*. Compared with serrated leaf margins in the wild type (Figures 8A to 8C), the leaf teeth in *nam-2* became relatively smooth, indicating that NAM is involved in the promotion of leaf margin serrations (Figures 8D to 8F). To investigate the roles of NAM in the formation of lobed leaf margin in *ago7-1,* an *ago7-1 nam-2* double mutant was generated (see Supplemental Figure 11 online). Compared with *ago7-1,* the degree of indentation in the leaf margin was decreased in the double mutant, confirming that NAM indeed positively regulates the formation of leaf margin serration (Figures 8G to 8K). These data further suggest that the *TAS3* ta-siRNA pathway and NAM antagonistically regulate the development of leaf margins in *M. truncatula*.

To further elucidate the genetic interaction between NAM and the *TAS3* ta-siRNA pathway, the developmental pattern of leaflets was examined. The adult leaves of the wild type exhibit trifoliate form. In *nam-2*, 82% of leaves were simplified because of fused leaflets. In contrast with *nam-2*, the frequency of fused leaflets in the *ago7-1 nam-2* was dramatically decreased to 5% (Figure 8L). Furthermore, the elongated rachis and petiole in *ago7-1* were suppressed in the double mutant (Figures 8M and 8N). These observations indicate that the *TAS3* ta-siRNA pathway and NAM also antagonistically regulate the separation of lateral leaflets.

Leaf Margin Development Regulated by NAM Is Dependent on SLM1

To determine whether NAM functions in concert with auxin polar transport to promote leaf margin serration development, a *nam-2 slm1-1* double mutant was generated (see Supplemental Figure 11 online). The leaf margin of the double mutant resembled that of *slm1-1*, indicating that leaf margin development regulated by

Figure 6. (continued).

(A) In situ hybridization of *ARF3* in leaf primordia of the wild type and *ago7-1*.
(B) A diagram represents the coding sequence of *ARF3*. The fragment used for $ARF3_{RNAi}$ and the two mutated *ta-siARF* target sites are shown.
(C) Transcript levels of *ARF3* in wild-type, mutant and transgenic plants. Values are the means and SD of three biological replicates. *P < 0.05; **P < 0.01.
(D) and **(E)** Adult leaves of the wild type **(D)** and *ago7-1* **(E)**.
(F) and **(G)** Adult leaves of *ago7-1* transgenic plants harboring the $ARF3_{RNAi}$ construct. The leaves at the vegetative stage **(F)** and reproductive stage **(G)** are shown.
(H) to **(M)** Adult leaves of transgenic plants overexpressing *ARF3* and *ARF3mut*. Leaves at the vegetative stage ([**H], [I], [K],** and [**L])** and reproductive stage **([J]** and **[M])** are shown. Arrows point to the downward-curled leaf margin in **(I)** and **(L)**.
(N) Transcript levels of the *ARF3* in the different regions (outer, middle, and inner) of leaflet in the wild type and *ago7-1*. Values are the means and SD of three biological replicates. *P < 0.05; **P < 0.01.
(O) *DR5:GUS* expression in developing leaflet of the wild type and *ago7-1*. Close views (empty boxes) of margin serrations in the wild type and *ago7-1* are shown on the right side.
AB, abaxial; AD, adaxial; P: plastochron; WT, wild type.
Bar in **(A)** = 50 μm; bar in **(D)** to **(M)** = 5 mm; bar in **(O)** = 1 mm.

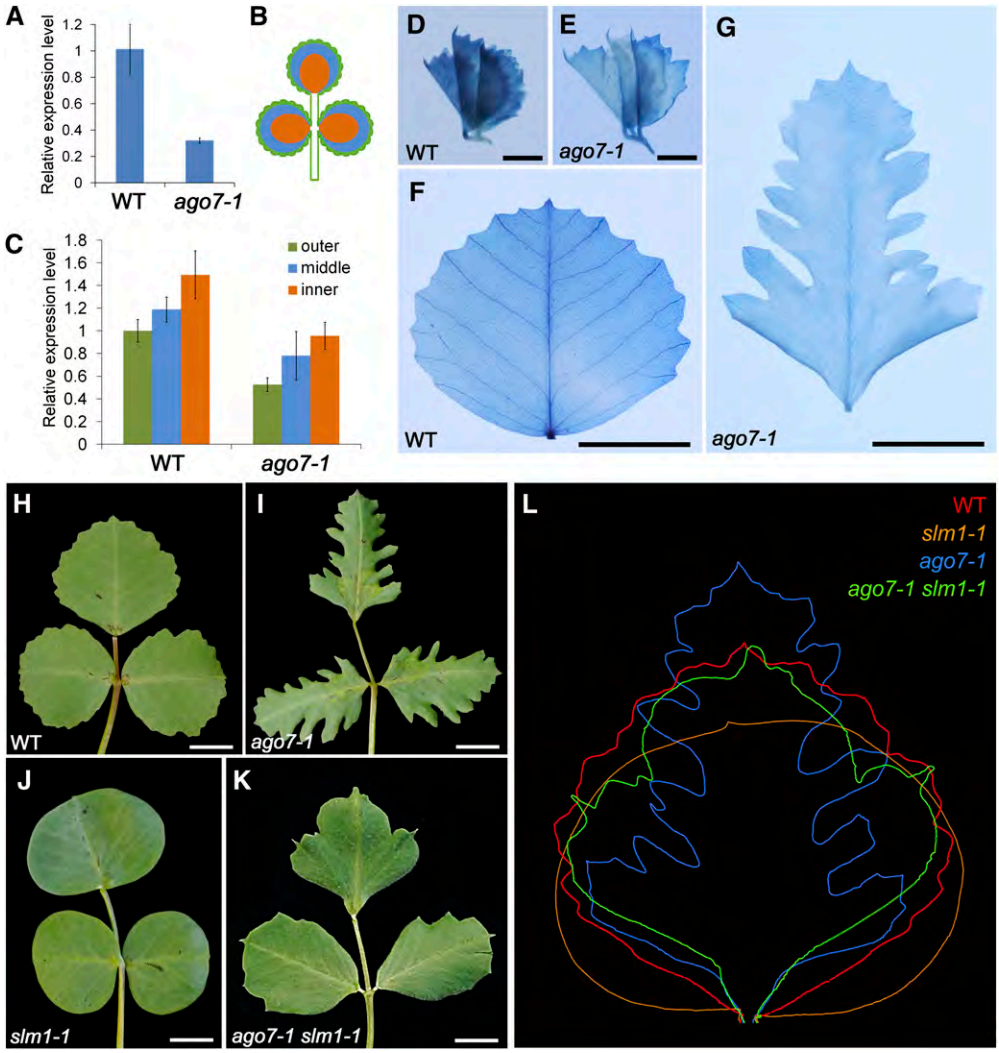

Figure 7. Formation of Lobed Leaf Margin in *ago7-1* Is Partially Dependent on SLM1 in *M. truncatula*.

(A) Transcript levels of *SLM1* in the wild type (WT) and *ago7-1*. Transcript levels were measured by qRT-PCR using leaves from 6-week-old plants. Values are the means and SD of three biological replicates.

(B) and **(C)** Transcript levels of *SLM1* in different regions of leaflets in the wild type **(B)** and *ago7-1* **(C)**. Values are the means and SD of three biological replicates.

(D) to **(G)** SLM1 expression pattern in leaf buds **([D]** and **[E])** and fully expanded terminal leaflet **([F]** and **[G])** of the wild type and *ago7-1*, as determined by detecting the *SLM1pro:GUS* activity.

(H) to **(K)** Adult leaves of the wild type **(H)**, *ago7-1* **(I)**, *slm1-1* **(J)**, and *ago7-1slm1-1* **(K)**.

(L) The outlines of terminal leaflets of the wild type (red), *ago7-1* (blue), *slm1-1* (khaki), and *ago7-1 slm1-1* (green) are overlapped.

Bar in **(D)** and **(E)** = 3 mm; bar in **(F)** to **(K)** = 5 mm.

NAM is dependent on SLM1 (Figures 9A to 9C). Moreover, the frequency of fused leaflets in the double mutant increased (Figure 9D), suggesting that NAM and SLM1 play redundant roles in the separation of leaflets. In addition, the transcript level of *NAM* was downregulated in *slm1-1* compared with that in the wild type (Figure 9E). The spatial localization of *NAM* in *slm1-1* was further examined by in situ hybridization (Figure 9F). Whereas *NAM* mRNA was easily detected in the developing leaf margins of the wild type, an obvious reduction in *NAM* expression in leaf margins of *slm1-1* was observed. The qRT-PCR and in situ hybridization results showed that proper auxin distribution is required for *NAM* expression.

DISCUSSION

The Conserved *TAS3* ta-siRNA Pathway Has Different Roles in Leaf Development

Arabidopsis AGO7 and its orthologs (*REL3* in *L. japonicus*, *WIRY2* in tomato, *SHOOTLESS4* in rice, and *RAGGED SEEDLING2* in

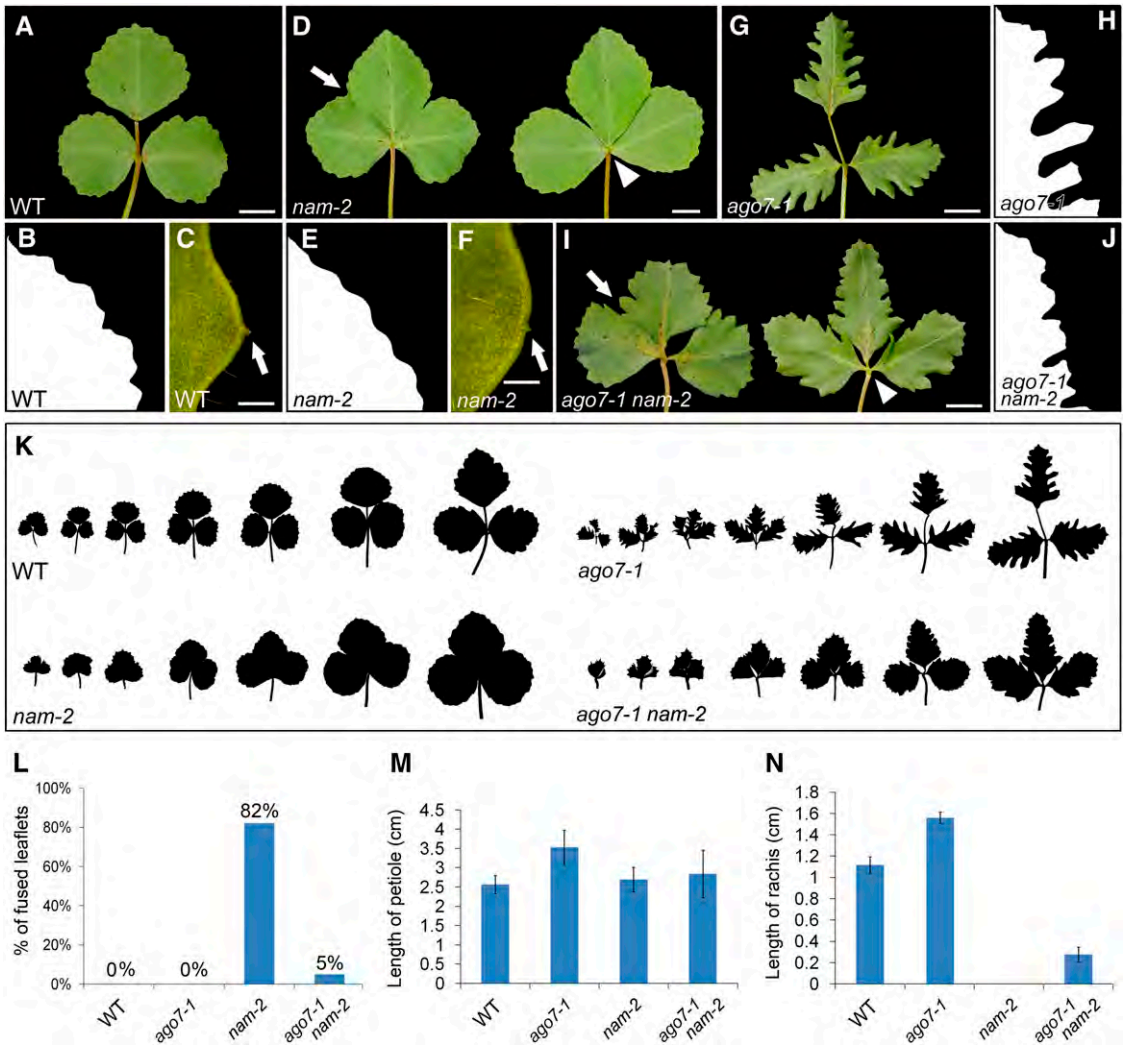

Figure 8. Interaction Between the *TAS3* ta-siRNA Pathway and NAM in Leaf Development in *M. truncatula*.

(A) to **(C)** Leaf margin phenotype of the wild type (WT). Arrow points to the tip of leaf margin serration.
(D) to **(F)** Leaf margin phenotype of *nam-2*. Arrows point to the fused leaflets in **(D)** and the relatively smooth leaf margin serration in **(F)**. Arrowhead marks the clustered leaflets without rachis in **(D)**.
(G) and **(H)** Adult leaves **(G)** and leaf margin **(H)** of *ago7-1*.
(I) and **(J)** Adult leaves **(I)** and leaf margin **(J)** of *ago7-1 nam-2*. Arrow indicates the fused leaflets. Arrowhead points to the clustered leaflets with partially recovered rachis.
(K) The leaf series of the wild type, *nam-2*, *ago7-1*, and *ago7-1nam-2*.
(L) Percentage of fused leaflets in the wild type and mutants (n = 50).
(M) and **(N)** Length of petiole **(M)** and rachis **(N)** of the wild type and mutants. The data were measured on the first fully expanded trifoliate of 6-week-old plants. Means ± SD are shown (n = 40).
Bar in **(A)**, **(D)**, **(G)**,and **(I)** = 5 mm; bar in **(C)** and **(F)** = 150 μm.

maize) have been shown to play key roles in the *TAS3* ta-siRNA pathway (Hunter et al., 2003; Nagasaki et al., 2007; Douglas et al., 2010; Yan et al., 2010; Yifhar et al., 2012). In this study, *AGO7* (*LOL1*) is identified as the *M. truncatula* ortholog of *Arabidopsis AGO7*. Three *ARF* genes were upregulated in *ago7*. These data further support that the regulation mechanism of the *TAS3* ta-siRNA pathway is well conserved in both dicots and monocots. Blocking of the *TAS3* ta-siRNA pathway has different effects on leaf pattern among species. For example, tomato *wiry2/ago7* alleles exhibited leaflet number variations at different developmental stages. *L. japonicus rel3* showed a reduced number of leaflets (Yan et al., 2010). By contrast, the leaflet number of adult leaves in both *ago7* and *OX-ARF3mut* plants did not change. Previous studies indicate that the leaf patterns of both tomato and *L. japonicus* are determined in response to the Class I *KNOTTED*-like homeobox (*KNOX1*) expression domain (Hareven

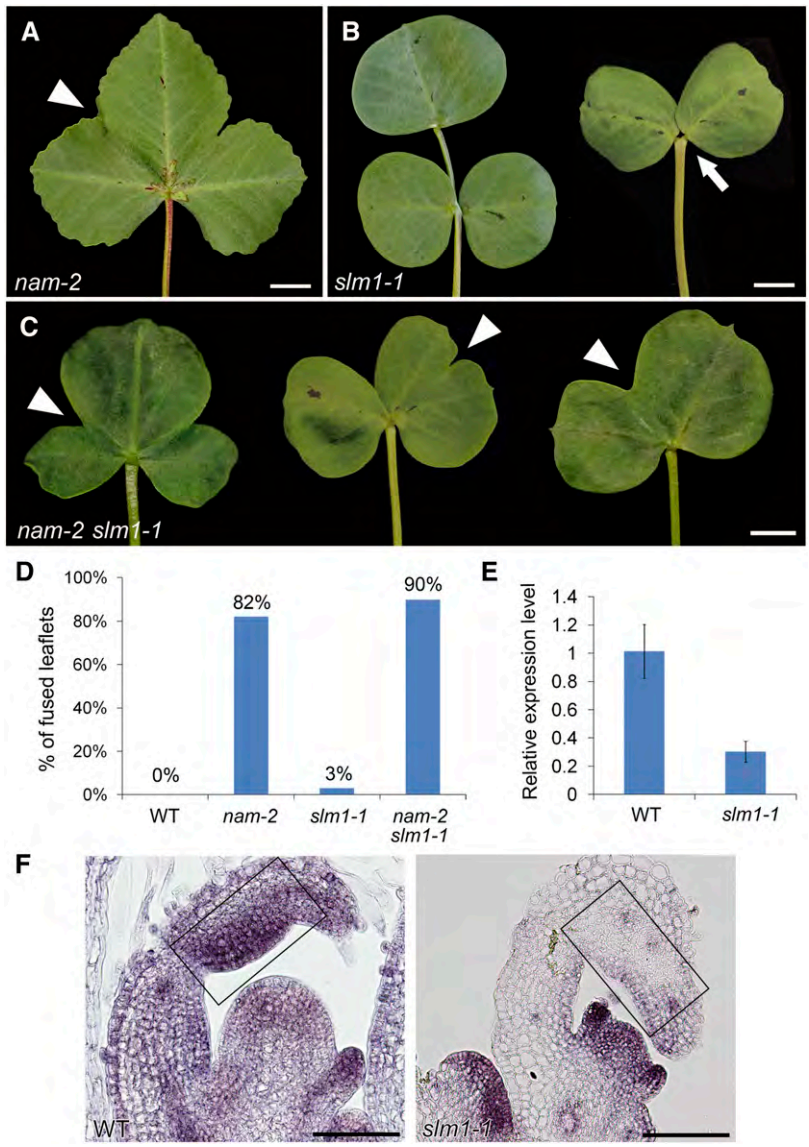

Figure 9. Leaf Margin Development Regulated by NAM Is Dependent on SLM1.

(A) to **(C)** Adult leaves of *nam-2* **(A)**, *slm1-1* **(B)**, and *nam-2 slm1-1* **(C)**. Arrow points to the clustered leaflets. Arrowheads indicate the fused leaflets.
(D) Percentage of fused leaflets in the 6-week-old wild type and mutants (n = 50).
(E) Transcript levels of *NAM* in the wild type (WT) and *slm1-1*. Transcript levels were measured by qRT-PCR using leaf buds from 6-week-old plants. Values are the means and SD of three biological replicates.
(F) In situ hybridization and expression patterns of *NAM* in leaf primordia of the wild type and *slm1-1*. Empty boxes mark the leaf margin.
Bar in **(A)** to **(C)** = 5 mm; bar in (**F**) = 50 μm.

et al., 1996; Champagne et al., 2007). *M. truncatula* belongs to the inverted repeat–lacking clade of legumes (Fabaceae), and *SINGLE LEAFLET1*, the *FLORICAULA/LEAFY* ortholog, functions in place of *KNOX1* to regulate compound leaf development (Wojciechowski et al., 2004; Champagne et al., 2007; Wang et al., 2008). It could be speculated that different determination mechanisms of compound leaf development result in diverse responses to the loss of ta-siRNA. The investigation and comparison of gene functions among species are critical for obtaining insight into the general or specialized gene functions (Efroni et al., 2010; Yifhar et al., 2012).

ARF3 Regulates Leaf Shape by Maintaining Proper Leaf Polarity

Mutants with defects on adaxial-abaxial polarity display filamentous organs, demonstrating the importance of boundary formation for morphogenesis (Townsley and Sinha, 2012; Nakata and

Okada, 2013). Leaf margin cells are a type of boundary cell that forms a specific structure to separate the adaxial and abaxial epidermis of the leaf blade. Such structures are required for proper leaf blade growth and are also regulated by leaf adaxial-abaxial polarity (Sarojam et al., 2010; Szakonyi et al., 2010; Wang et al., 2011; Yamaguchi et al., 2012; Nakata and Okada, 2013). In this study, the dorsiventral polarity of the leaf is altered in *ago7* as a result of the ectopic expression of *ARF3*. In accordance with the polarity defects, the development of leaf margin cells is also abnormal as evidenced by the loss of their cell identity. Therefore, by regulating the establishment of leaf polarity, *ARF3* is probably indirectly involved in the formation of leaf margin cells. On the other hand, the pattern of cell proliferation and expansion is a major factor affecting organ shape (Nakata and Okada, 2013). Accompanying the defects in margin cell identity in *ago7*, the density of margin cells was increased and the cell size was decreased in the sinus of the leaf margin, suggesting that both cell proliferation and expansion are changed. Such irregular cell development results in the overgrowth of leaf margin teeth, which finally promotes the formation of lobed leaf margins.

The *TAS3* ta-siRNA Pathway and the Auxin/SLM1 Module Play Essential but Different Roles in Leaf Margin Formation in *M. truncatula*

Auxin is known as the key hormone for elaboration of leaf margins (Hay et al., 2006; Barkoulas et al., 2008; Koenig et al., 2009; Bilsborough et al., 2011; Zhou et al., 2011a). The differential distribution of auxin between cells of a tissue is crucial for auxin-mediated developmental processes (Vanneste and Friml, 2009; Byrne, 2012). Based on the expression of *DR5* reporter constructs, auxin responsiveness was altered along the leaf margin of *ago7*. It has been suggested that auxin distribution is dependent on the dorsiventral pattern (Zgurski et al., 2005; Nakata and Okada, 2013). Therefore, the increased auxin response in *ago7* is likely a result of the changed leaf polarity induced by ectopic expression of *ARF3*. In turn, *ARF3* is implicated in leaf development by responding to auxin signaling (Pekker et al., 2005). Taken together, these findings imply that crosstalk between the *TAS3* ta-siRNA pathway and auxin distribution probably exists during leaf margin formation (Figure 10).

In *M. truncatula*, loss of function of SLM1 results in the smooth leaf margin (Zhou et al., 2011a). In contrast with *slm1*, the *slm1 ago7* double mutant formed serrations (Figure 7). The *TAS3* ta-siRNA pathway represses the degree of indentation by suppressing the expression of *ARF3*. Such regulation is independent of the SLM1-mediated mechanism but could be enhanced by the auxin/SLM1 module. This is evidenced by the observation that the degree of indentation in *slm1 ago7* is not as pronounced as *ago7*, although the SLM1 expression is partially repressed in *ago7* (see Supplemental Figures 6J and 10B online). These data suggest that elaboration of leaf margin formation requires two different processes and corresponding regulators: (1) the auxin/SLM1 module regulates the initiation of leaf margin teeth; and (2) the *TAS3* ta-siRNA pathway determines the degree of marginal indentation (Figure 10).

The *TAS3* ta-siRNA Pathway and NAM Antagonistically Regulate the Degree of Indentation of Leaf Margin in a Context-Dependent Manner

Leaf margin patterning is dependent on genetic networks involving transcription factors and hormone signaling (Byrne, 2012). A recent study proposes a fine model of the interdependent feedback loops among PIN1, CUC2, and auxin distribution. In this model, proper auxin activity gradients established by both CUC2 and PIN1 are required for producing regularly spaced marginal serrations (Bilsborough et al., 2011). As a result, the *pin1* and *cuc2* loss of function mutants fail to form teeth in *Arabidopsis*. In *M. truncatula*, auxin maxima established by SLM1 at the teeth tips is crucial for the formation of leaf serrations (Zhou et al., 2011a). Leaf margin development is also partially dependent on NAM. Unlike the smooth leaf margin of *cuc2* in *Arabidopsis*, *nam-2* still developed a less serrated leaf margin. This finding does not contradict the conserved roles of NAM in the initiation of leaf margin teeth because *nam-2* is a weak allele. The *slm1 nam* double mutant showed a smooth leaf margin, indicating that NAM is dependent on SLM1 to promote leaf serrations. In addition, the expression of *NAM* varied with auxin distribution as revealed by the repression of *NAM* in *slm1*. These data indicate that NAM and

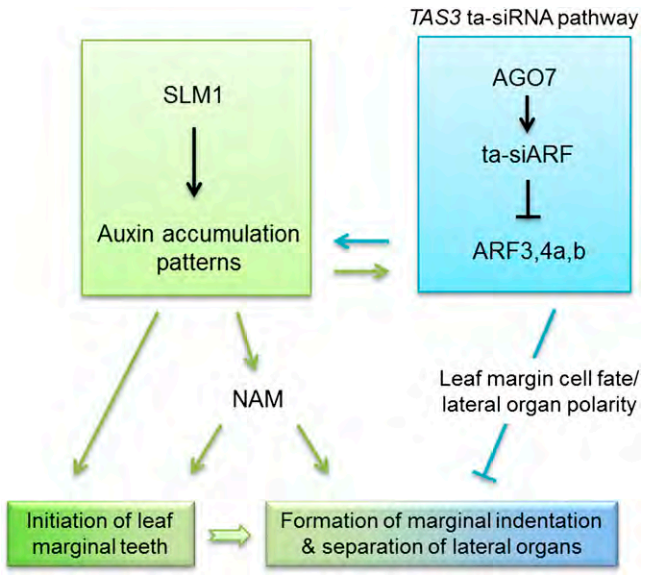

Figure 10. A Proposed Model Illustrating the Functional Roles of the *TAS3* ta-siRNA Pathway, NAM, and SLM1 in Leaf Margin Development and Lateral Organ Separation.

SLM1 is an auxin efflux carrier that regulates auxin accumulation during leaf development. The auxin/SLM1 module is required for the initiation of leaf marginal teeth. NAM is a positive regulator that promotes the formation of leaf margin serrations and the separation of lateral organs in a SLM1-dependent manner. AGO7 is required for the production of *ta-siARFs*, which repress the expression of *ARF3* and *ARF4a,b* by posttranscriptional cleavage in the *TAS3* ta-siRNA pathway. The *TAS3* ta-siRNA pathway plays crucial roles in the determination of leaf margin cell fate and the establishment of lateral organ polarity. It functions as a repressor in the formation of marginal indentation and separation of lateral organs.

SLM1 play conserved roles in the regulation of leaf marginal structure in *M. truncatula*. It was proposed that the relative balance between growth promotion and growth repression results in the ultimate leaf shape (Byrne, 2012). In *M. truncatula*, a growth balance was observed in the elaboration of leaf margins. On one side, the *TAS3* ta-siRNA pathway represses the degree of indentation at the leaf margin by suppressing *ARF3*. On the other side, NAM promotes the formation of leaf serrations in an auxin-dependent manner. These observations suggest that the *TAS3* ta-siRNA pathway and NAM antagonistically act on the elaboration of leaf margin serrations (Figure 10).

Different plant species exhibit large variations in leaf shape. For example, both *Arabidopsis* and *M. truncatula* display serrated leaves, whereas the entire leaf margin in *L. japonicus* is without teeth. Although the *TAS3* ta-siRNA regulation mechanism is highly conserved, blocking the synthesis of *TAS3* ta-siRNAs did not yield the same phenotypic changes in leaf margin among species. In *Arabidopsis*, *ago7* shows elongated leaves with increased serrations in the leaf margin (Hunter et al., 2003). In *M. truncatula*, leaf serrations are strongly enhanced to form leaf lobing in *ago7*. However, in *L. japonicus*, the *TAS3* ta-siRNA pathway–related mutants, *rel1* and *rel3*, show smooth leaf margins similar to the wild type, although the leaf polarity changed dramatically (Yan et al., 2010). It seems that the role of the *TAS3* ta-siRNA pathway in leaf margin morphogenesis depends on the prior state of competence. These observations are reminiscent of the different context-specific developmental events when KNOX1 is expressed ectopically in compound leaf species and simple leaf species (Efroni et al., 2010). For example, the ectopic activity of KNOX1 causes a substantial increase in leaflet number in tomato but leads to lobed leaves, rather than induction of leaflets, in *Arabidopsis* (Shani et al., 2009). Therefore, the distinct developmental identities of leaf margins among species imply that the regulation of leaf shape by the *TAS3* ta-siRNA pathway is species specific. We propose a possible regulation mechanism in which the *TAS3* ta-siRNA pathway influences leaf margin development in a species-specific manner by interacting with SLM1 and NAM through the auxin patterning and signaling pathway (Figure 10).

METHODS

Plant Materials and Growth Conditions

Medicago truncatula ecotype R108 was used in this study. NF3499 (*ago7-1*), NF6270 (*ago7-2*), NF6665 (*ago7-3*), and NF4633 (*ago7-4*) mutant lines were identified from a *Tnt1* retrotransposon-tagged mutant collection of *M. truncatula* (Tadege et al., 2008). Plants were grown at 24°C (day) and 20°C (night), 16-h day and 8-h night photoperiods, 70 to 80% relative humidity, and 150 μmol/m^2/s light intensity.

Molecular Cloning of *AGO7* and Identification of Insertion Sites in *AGO7*

Thermal asymmetric interlaced PCR was performed as previously described (Tadege et al., 2008). PCR and RT-PCR were performed to amplify the *AGO7* genomic DNA sequence and *AGO7* CDS sequence. The *Tnt1* or *Mere1* retrotransposon flanking sequences from *ago7-2, ago7-3*, and *ago7-4* were PCR amplified (MJ Research PTC-200 Thermal Cycler) using a combination of *Tnt1*- or *Mere1*-specific primer and *AGO7* gene-specific primer (see Supplemental Data Set 5 online). The PCR products were purified and cloned into pGEM-T Easy vector (Promega) for sequencing, and the sequences were aligned (NCBI blastn: Align two or more sequences) with the *AGO7* genomic DNA sequence to determine the retrotransposon insertion sites.

Microscopy and Photography

Leaves and flowers at different stages were collected. For scanning electron microscopy analysis, sample fixation was performed as previously described (Zhou et al., 2011a). The Hitachi TM-3000 Tabletop Scanning Electron Microscope was used for observation. For fluorescence imaging, samples were observed with a Leica TCS SP2 AOBS confocal laser scanning microscope using the 488-nm line of an argon laser for the GFP signal, and emission was detected at 510 nm (Leica Microsystems). The silhouettes in Figure 8 were produced by Adobe Photoshop CS5 software. The original photos were adjusted using the commands levels and brightness/contrast, and then changed to black/white using the command black and white.

Histology, GUS Staining, and Pollen Staining

The adult leaves and petioles were fixed in 3% glutaraldehyde in a phosphate buffer. Dehydrated samples were embedded in LR white resin (London Resin). Sample sectioning and staining were performed as previously described (Zhou et al., 2011a). Leaf buds and fully expanded leaves were collected for GUS staining. GUS activity was histochemically detected as previously described (Jefferson et al., 1987). To determine pollen viability, flowers of the wild type and *ago7-1* were collected. Sample staining was performed as previously described (Zhou et al., 2011a).

In Situ Hybridization Analysis

The fragments of 525-bp *AGO7*, 621-bp *ARF3*, and 638-bp *NAM* CDS were amplified by PCR. The PCR product was labeled with digoxigenin-11-UTP (Roche Diagnostics). RNA in situ hybridization was performed on shoot apices or inflorescence apices of 4-wk-old wild-type or *slm1-1* plants as previously described (Zhou et al., 2011a).

Plasmids and Plant Transformation

To obtain the *SLM1* genomic clone for functional complementation of the *ago7* mutant, the 2.5-kb promoter sequence plus 4.2-kb *AGO7* genomic sequence was amplified using the primers AGO7-PRO-F and AGO7-PRO-R, and transferred into the Gateway plant transformation destination vector pEarleyGate 301 (Earley et al., 2006) using the Gateway LR reaction (Invitrogen). To generate the *AGO7* overexpression construct, the CDS of *AGO7* was amplified using the primers AGO7-CDS-F and AGO7-CDS-R (see Supplemental Data Set 5 online). The PCR product was purified and cloned into pEarleyGate 100 (Earley et al., 2006). To construct the $ARF3_{RNAi}$ vector, a 602-bp fragment of *ARF3* CDS was PCR amplified from wild-type *M. truncatula* and transferred into the Gateway plant transformation destination vector pANDA35K. To construct the *ARF3* overexpression vector, *ARF3* CDS was PCR amplified and transferred into pEarleyGate 100. To construct the *ARF3mut* overexpression vector, silent mutations were introduced into two *ta-siARF* target sites of *ARF3* CDS using the QuikChange II Site-Directed Mutagenesis Kit (Stratagene) and then transferred into pEarleyGate 100 vector. The *DR5rev:GFP* reporter construct was previously described (Zhou et al., 2011a). The leaves of *M. truncatula ago7-1* and the wild type were transformed with the *Agrobacterium tumefaciens* EHA105 strain harboring the various destination vectors (Cosson et al., 2006; Crane et al., 2006).

Phylogenetic Analysis

The protein sequences of ARGONAUTE family members and ARF RESPONSE FACTOR family members were used for phylogenetic

analysis. Alignments were performed using ClustalW2 with default parameters (alignment type, slow; protein weight matrix, gonnet; gap open, 10; gap extension, 0.1). A phylogenetic tree was constructed by MEGA4 using the neighbor-joining method with 1000 bootstrap replications (http://www.megasoftware.net/).

RNA Extraction, RT-PCR, qRT-PCR, and Microarray Analysis

The shoot meristem tissues of 4-wk-old wild-type and mutant plants were collected for RNA isolation. Total RNA was extracted using the RNeasy Plant Mini Kit (Qiagen) and cleaned with the DNA-free Kit (Ambion). cDNA synthesis for RT-PCR and real-time RT-PCR was performed using SuperScript III reverse transcriptase (Invitrogen) as previously described (Zhou et al., 2011a). For qRT-PCR, triplicate biological samples were collected. SYBR Green (Sigma-Aldrich) was used as the reporter dye. qRT-PCR was performed with an ABI PRISM 7900 HT sequence detection system (Applied Biosystems). Data were analyzed using the SDS 2.2.1 software (Applied Biosystems). The protocol for the amplification and detection of *ta-siARF* was adapted from a previous report (Varkonyi-Gasic et al., 2007). The stem-loop reverse transcription primers and *ta-siARF*–specific and miR390-specific PCR primers were designed and used for RT-PCR. Primer sequences used are listed in Supplemental Data Set 5 online.

For microarray analysis, *ago7-1* mutants and wild-type–like plants in a segregating F2 population were used. Shoot apices of 4-wk-old plants were collected from triplicate biological replicates of the above samples for RNA extraction. RNA purification, probe labeling, hybridization, and scanning for microarray analysis were conducted as previously described (Zhou et al., 2011b). Data normalization between chips was conducted using the robust multichip average technique (Irizarry et al., 2003). Presence/absence calls for each probe set were obtained using dChip software (Li and Wong, 2001). Gene selections for pairwise comparison were made based on associative analysis (Dozmorov and Centola, 2003) in Matlab software (MathWorks). In this method, the background noise presented between replicates and technical noise during microarray experiments were measured by the residual presented among a group of genes whose residuals are homoscedastic. Genes whose residuals between the compared sample pairs that were significantly higher than the measured background noise level were considered to be differentially expressed. A selection threshold of 2 for transcript ratios and a Bonferroni-corrected P-value threshold of 8.15954E-07 were used. The Bonferroni-corrected P-value threshold was derived from 0.05/*n* in these analyses, where *n* is the number of probe sets (61,278) on the chip, in order to correct the family-wide false discovery rate (Abdi, 2007).

Generation of Double Mutants

The *ago7-1, slm1-1*, and *nam-2* heterozygous plants were used as parents and crossed with each other to generate F1 plants. F1 plants were genotyped by PCR to identify heterozygotes, which were then selfed to generate F2 plants. The double phenotype was identified in a segregating population and was confirmed by PCR.

Accession Numbers

Sequence data from this article can be found in the National Center for Biotechnology Information GenBank, *Medicago truncatula* Hapmap Project, or miRBase under the following accession numbers: Mt-AGO7 (XM_003613868), At-AGO7 (AT1G69440), Os-AGO7 (OS03G0449200), SLM1 (AAT48630), NAM (JF929904), Mt-ARF3 (Medtr2g014770.1), Mt-ARF4a (Medtr4g060470.1), ARF4b (Medtr2g093740.1), At-ARF3 (At2g33860), ARF4 (At5g60450), and miR390 (MIMAT0011072).

Supplemental Data

The following materials are available in the online version of this article.

Supplemental Figure 1. Complementation of *ago7-1* by AGO7 and Overexpression of AGO7 in the Wild Type.

Supplemental Figure 2. Phylogenetic Tree and Alignment of Mt-AGO7 with Other Members of the ARGONAUTE Family.

Supplemental Figure 3. Phylogenetic Relationships of ARF Proteins in *M. truncatula, Arabidopsis*, and Rice.

Supplemental Figure 4. Expression Profiling of the *ARF3*, *ARF4a*, and *ARF4b* Transcripts.

Supplemental Figure 5. The Relative Expression Level of Three *ARF* Genes in the Wild Type and *ago7-1*.

Supplemental Figure 6. Leaf Margin Development in the Wild Type and *ago7-1*.

Supplemental Figure 7. Relative Expression Level of *ARF4a* and *ARF4b* in Leaves of the Wild Type, *ago7-1*, and $ARF3_{RNAi}$ *ago7-1*.

Supplemental Figure 8. Auxin Distribution in the Wild Type and *ago7-1*.

Supplemental Figure 9. Relative Expression Level of *ARF3* in Leaves Treated with Auxin.

Supplemental Figure 10. Phenotype of Leaf Margin at the Early Developmental Stage.

Supplemental Figure 11. Phenotype of 40-d-Old Plants of the Wild Type and Mutants.

Supplemental Table 1. Analysis of Leaf Growth in *ago7-1* Mutant, Wild-Type, and Transgenic Plants.

Supplemental Data Set 1. Alignment Used to Generate the Phylogeny Presented in Supplemental Figure 2.

Supplemental Data Set 2. Genes Upregulated More Than Twofold in *ago7-1* Mutants Compared with Those of the Wild Type.

Supplemental Data Set 3. Genes Downregulated More Than Twofold in *ago7-1* Mutants Compared with Those of the Wild Type.

Supplemental Data Set 4. Alignment Used to Generate the Phylogeny Presented in Supplemental Figure 3.

Supplemental Data Set 5. Primers Used in This Study.

ACKNOWLEDGMENTS

The authors thank Amy Mason, Jackie Kelley, and Katie Wenzell for critical reading of the article, greenhouse staff for assistance with plant care, and the Samuel Roberts Noble Electron Microscopy Laboratory for the scanning electron microscopy work. This work was supported by the Samuel Roberts Noble Foundation, the National Science Foundation (Grant EPS-0814361), and the BioEnergy Science Center. The BioEnergy Science Center is a U.S. Department of Energy Bioenergy Research Center supported by the Office of Biological and Environmental Research in the Department of Energy Office of Science.

AUTHOR CONTRIBUTIONS

C.Z. and Z.-Y.W. designed the research. C.Z., L.H., C.F., X.C., J.N., J.M., and Y.T an performed the experiments. C.Z., L.H., J.W., Y. Tang, G.X., and Z.-Y.W. analyzed the data. M.T. and K.S.M. contributed analytical tools. C.Z. and Z.W. wrote the article.

Received August 22, 2013; revised November 22, 2013; accepted December 6, 2013; published December 24, 2013.

REFERENCES

Abdi, H. (2007). Bonferroni and Sidak corrections for multiple comparisons. In Encyclopedia of Measurement and Statistics, N.J. Salkind, ed. (Thousand Oaks, California: Sage), pp. 103–107.

Adenot, X., Elmayan, T., Lauressergues, D., Boutet, S., Bouché, N., Gasciolli, V., and Vaucheret, H. (2006). DRB4-dependent TAS3 trans-acting siRNAs control leaf morphology through AGO7. Curr. Biol. **16:** 927–932.

Aida, M., and Tasaka, M. (2006). Genetic control of shoot organ boundaries. Curr. Opin. Plant Biol. **9:** 72–77.

Allen, E., Xie, Z., Gustafson, A.M., and Carrington, J.C. (2005). microRNA-directed phasing during trans-acting siRNA biogenesis in plants. Cell **121:** 207–221.

Barkoulas, M., Hay, A., Kougioumoutzi, E., and Tsiantis, M. (2008). A developmental framework for dissected leaf formation in the *Arabidopsis* relative *Cardamine hirsuta*. Nat. Genet. **40:** 1136–1141.

Benlloch, R., Navarro, C., Beltran, J.P., and Canas, L.A. (2003). Floral development of the model legume *Medicago truncatula*: Ontogeny studies as a tool to better characterize homeotic mutations. Sex. Plant Reprod. **15:** 231–241.

Berger, Y., Harpaz-Saad, S., Brand, A., Melnik, H., Sirding, N., Alvarez, J.P., Zinder, M., Samach, A., Eshed, Y., and Ori, N. (2009). The NAC-domain transcription factor GOBLET specifies leaflet boundaries in compound tomato leaves. Development **136:** 823–832.

Bilsborough, G.D., Runions, A., Barkoulas, M., Jenkins, H.W., Hasson, A., Galinha, C., Laufs, P., Hay, A., Prusinkiewicz, P., and Tsiantis, M. (2011). Model for the regulation of *Arabidopsis thaliana* leaf margin development. Proc. Natl. Acad. Sci. USA **108:** 3424–3429.

Blein, T., Pulido, A., Vialette-Guiraud, A., Nikovics, K., Morin, H., Hay, A., Johansen, I.E., Tsiantis, M., and Laufs, P. (2008). A conserved molecular framework for compound leaf development. Science **322:** 1835–1839.

Braybrook, S.A., and Kuhlemeier, C. (2010). How a plant builds leaves. Plant Cell **22:** 1006–1018.

Byrne, M.E. (2012). Making leaves. Curr. Opin. Plant Biol. **15:** 24–30.

Champagne, C.E., Goliber, T.E., Wojciechowski, M.F., Mei, R.W., Townsley, B.T., Wang, K., Paz, M.M., Geeta, R., and Sinha, N.R. (2007). Compound leaf development and evolution in the legumes. Plant Cell **19:** 3369–3378.

Cheng, X., Peng, J., Ma, J., Tang, Y., Chen, R., Mysore, K.S., and Wen, J. (2012). *NO APICAL MERISTEM* (*MtNAM*) regulates floral organ identity and lateral organ separation in *Medicago truncatula.* New Phytol. **195:** 71–84.

Cosson, V., Durand, P., d'Erfurth, I., Kondorosi, A., and Ratet, P. (2006). *Medicago truncatula* transformation using leaf explants. Methods Mol. Biol. **343:** 115–127.

Crane, C., Wright, E., Dixon, R.A., and Wang, Z.Y. (2006). Transgenic *Medicago truncatula* plants obtained from *Agrobacterium tumefaciens*-transformed roots and *Agrobacterium rhizogenes*-transformed hairy roots. Planta **223:** 1344–1354.

DeMason, D.A., and Chawla, R. (2004). Roles for auxin during morphogenesis of the compound leaves of pea (*Pisum sativum*). Planta **218:** 435–448.

Douglas, R.N., Wiley, D., Sarkar, A., Springer, N., Timmermans, M.C., and Scanlon, M.J. (2010). ragged seedling2 encodes an ARGONAUTE7-like protein required for mediolateral expansion, but not dorsiventrality, of maize leaves. Plant Cell **22:** 1441–1451.

Dozmorov, I., and Centola, M. (2003). An associative analysis of gene expression array data. Bioinformatics **19:** 204–211.

Earley, K.W., Haag, J.R., Pontes, O., Opper, K., Juehne, T., Song, K., and Pikaard, C.S. (2006). Gateway-compatible vectors for plant functional genomics and proteomics. Plant J. **45:** 616–629.

Efroni, I., Eshed, Y., and Lifschitz, E. (2010). Morphogenesis of simple and compound leaves: A critical review. Plant Cell **22:** 1019–1032.

Fahlgren, N., Montgomery, T.A., Howell, M.D., Allen, E., Dvorak, S.K., Alexander, A.L., and Carrington, J.C. (2006). Regulation of AUXIN RESPONSE FACTOR3 by TAS3 ta-siRNA affects developmental timing and patterning in *Arabidopsis*. Curr. Biol. **16:** 939–944.

Garcia, D., Collier, S.A., Byrne, M.E., and Martienssen, R.A. (2006). Specification of leaf polarity in *Arabidopsis* via the trans-acting siRNA pathway. Curr. Biol. **16:** 933–938.

Guilfoyle, T.J., and Hagen, G. (2001). Auxin response factors. J. Plant Growth Regul. **10:** 281–291.

Hareven, D., Gutfinger, T., Parnis, A., Eshed, Y., and Lifschitz, E. (1996). The making of a compound leaf: Genetic manipulation of leaf architecture in tomato. Cell **84:** 735–744.

Hay, A., Barkoulas, M., and Tsiantis, M. (2006). ASYMMETRIC LEAVES1 and auxin activities converge to repress BREVIPEDICELLUS expression and promote leaf development in *Arabidopsis*. Development **133:** 3955–3961.

Hunter, C., Sun, H., and Poethig, R.S. (2003). The *Arabidopsis* heterochronic gene ZIPPY is an ARGONAUTE family member. Curr. Biol. **13:** 1734–1739.

Hunter, C., Willmann, M.R., Wu, G., Yoshikawa, M., de la Luz Gutiérrez-Nava, M., and Poethig, S.R. (2006). Trans-acting siRNA-mediated repression of ETTIN and ARF4 regulates heteroblasty in *Arabidopsis*. Development **133:** 2973–2981.

Irizarry, R.A., Bolstad, B.M., Collin, F., Cope, L.M., Hobbs, B., and Speed, T.P. (2003). Summaries of Affymetrix GeneChip probe level data. Nucleic Acids Res. **31:** e15.

Jefferson, R.A., Kavanagh, T.A., and Bevan, M.W. (1987). GUS fusions: beta-Glucuronidase as a sensitive and versatile gene fusion marker in higher plants. EMBO J. **6:** 3901–3907.

Juarez, M.T., Twigg, R.W., and Timmermans, M.C. (2004). Specification of adaxial cell fate during maize leaf development. Development **131:** 4533–4544.

Koenig, D., Bayer, E., Kang, J., Kuhlemeier, C., and Sinha, N. (2009). Auxin patterns *Solanum lycopersicum* leaf morphogenesis. Development **136:** 2997–3006.

Li, C., and Wong, W.H. (2001). Model-based analysis of oligonucleotide arrays: Expression index computation and outlier detection. Proc. Natl. Acad. Sci. USA **98:** 31–36.

Liscum, E., and Reed, J.W. (2002). Genetics of Aux/IAA and ARF action in plant growth and development. Plant Mol. Biol. **49:** 387–400.

Liu, B., et al. (2007). *Oryza sativa* dicer-like4 reveals a key role for small interfering RNA silencing in plant development. Plant Cell **19:** 2705–2718.

Montgomery, T.A., Howell, M.D., Cuperus, J.T., Li, D., Hansen, J. E., Alexander, A.L., Chapman, E.J., Fahlgren, N., Allen, E., and Carrington, J.C. (2008). Specificity of ARGONAUTE7-miR390 interaction and dual functionality in TAS3 trans-acting siRNA formation. Cell **133:** 128–141.

Nagasaki, H., Itoh, J., Hayashi, K., Hibara, K., Satoh-Nagasawa, N., Nosaka, M., Mukouhata, M., Ashikari, M., Kitano, H., Matsuoka, M., Nagato, Y., and Sato, Y. (2007). The small interfering RNA production pathway is required for shoot meristem initiation in rice. Proc. Natl. Acad. Sci. USA **104:** 14867–14871.

Nakata, M., and Okada, K. (2013). The leaf adaxial-abaxial boundary and lamina growth. Plants **2:** 174–202.

Nogueira, F.T., Madi, S., Chitwood, D.H., Juarez, M.T., and Timmermans, M.C. (2007). Two small regulatory RNAs establish opposing fates of a developmental axis. Genes Dev. **21:** 750–755.

Pekker, I., Alvarez, J.P., and Eshed, Y. (2005). Auxin response factors mediate *Arabidopsis* organ asymmetry via modulation of KANADI activity. Plant Cell **17:** 2899–2910.

Rakocevic, A., Mondy, S., Tirichine, L., Cosson, V., Brocard, L., Iantcheva, A., Cayrel, A., Devier, B., Abu El-Heba, G.A., and Ratet, P. (2009). MERE1, a low-copy-number copia-type retroelement in *Medicago truncatula* active during tissue culture. Plant Physiol. **151:** 1250–1263.

Rast, M.I., and Simon, R. (2008). The meristem-to-organ boundary: More than an extremity of anything. Curr. Opin. Genet. Dev. **18:** 287–294.

Reinhardt, D., Pesce, E.R., Stieger, P., Mandel, T., Baltensperger, K., Bennett, M., Traas, J., Friml, J., and Kuhlemeier, C. (2003). Regulation of phyllotaxis by polar auxin transport. Nature **426:** 255–260.

Sarojam, R., Sappl, P.G., Goldshmidt, A., Efroni, I., Floyd, S.K., Eshed, Y., and Bowman, J.L. (2010). Differentiating *Arabidopsis* shoots from leaves by combined YABBY activities. Plant Cell **22:** 2113–2130.

Shani, E., Burko, Y., Ben-Yaakov, L., Berger, Y., Amsellem, Z., Goldshmidt, A., Sharon, E., and Ori, N. (2009). Stage-specific regulation of *Solanum lycopersicum* leaf maturation by class 1 KNOTTED1-LIKE HOMEOBOX proteins. Plant Cell **21:** 3078–3092.

Szakonyi, D., Moschopoulos, A., and Byrne, M.E. (2010). Perspectives on leaf dorsoventral polarity. J. Plant Res. **123:** 281–290.

Tadege, M., Wen, J., He, J., Tu, H., Kwak, Y., Eschstruth, A., Cayrel, A., Endre, G., Zhao, P.X., Chabaud, M., Ratet, P., and Mysore, K.S. (2008). Large-scale insertional mutagenesis using the Tnt1 retrotransposon in the model legume *Medicago truncatula.* Plant J. **54:** 335–347.

Timmermans, M.C., Schultes, N.P., Jankovsky, J.P., and Nelson, T. (1998). Leafbladeless1 is required for dorsoventrality of lateral organs in maize. Development **125:** 2813–2823.

Tiwari, S.B., Wang, X.J., Hagen, G., and Guilfoyle, T.J. (2001). AUX/IAA proteins are active repressors, and their stability and activity are modulated by auxin. Plant Cell **13:** 2809–2822.

Townsley, B.T., and Sinha, N.R. (2012). A new development: Evolving concepts in leaf ontogeny. Annu. Rev. Plant Biol. **63:** 535–562.

Ulmasov, T., Hagen, G., and Guilfoyle, T.J. (1999). Dimerization and DNA binding of auxin response factors. Plant J. **19:** 309–319.

Ulmasov, T., Murfett, J., Hagen, G., and Guilfoyle, T.J. (1997). Aux/IAA proteins repress expression of reporter genes containing natural and highly active synthetic auxin response elements. Plant Cell **9:** 1963–1971.

Vanneste, S., and Friml, J. (2009). Auxin: A trigger for change in plant development. Cell **136:** 1005–1016.

Varkonyi-Gasic, E., Wu, R., Wood, M., Walton, E.F., and Hellens, R.P. (2007). Protocol: A highly sensitive RT-PCR method for detection and quantification of microRNAs. Plant Methods **3:** 12.

Vernoux, T., Kronenberger, J., Grandjean, O., Laufs, P., and Traas, J. (2000). PIN-FORMED 1 regulates cell fate at the periphery of the shoot apical meristem. Development **127:** 5157–5165.

Wang, H., Chen, J., Wen, J., Tadege, M., Li, G., Liu, Y., Mysore, K.S., Ratet, P., and Chen, R. (2008). Control of compound leaf development by FLORICAULA/LEAFY ortholog SINGLE LEAFLET1 in *Medicago truncatula.* Plant Physiol. **146:** 1759–1772.

Wang, W., Xu, B., Wang, H., Li, J., Huang, H., and Xu, L. (2011). YUCCA genes are expressed in response to leaf adaxial-abaxial juxtaposition and are required for leaf margin development. Plant Physiol. **157:** 1805–1819.

Wojciechowski, M.F., Lavin, M., and Sanderson, M.J. (2004). A phylogeny of legumes (Leguminosae) based on analysis of the plastid matK gene resolves many well-supported subclades within the family. Am. J. Bot. **91:** 1846–1862.

Yamaguchi, T., Nukazuka, A., and Tsukaya, H. (2012). Leaf adaxial-abaxial polarity specification and lamina outgrowth: Evolution and development. Plant Cell Physiol. **53:** 1180–1194.

Yan, J., Cai, X., Luo, J., Sato, S., Jiang, Q., Yang, J., Cao, X., Hu, X., Tabata, S., Gresshoff, P.M., and Luo, D. (2010). The REDUCED LEAFLET genes encode key components of the trans-acting small interfering RNA pathway and regulate compound leaf and flower development in *Lotus japonicus*. Plant Physiol. **152:** 797–807.

Yifhar, T., Pekker, I., Peled, D., Friedlander, G., Pistunov, A., Sabban, M., Wachsman, G., Alvarez, J.P., Amsellem, Z., and Eshed, Y. (2012). Failure of the tomato *trans*-acting short interfering RNA program to regulate AUXIN RESPONSE FACTOR3 and ARF4 underlies the wiry leaf syndrome. Plant Cell **24:** 3575–3589.

Yoshikawa, M., Peragine, A., Park, M.Y., and Poethig, R.S. (2005). A pathway for the biogenesis of trans-acting siRNAs in *Arabidopsis*. Genes Dev. **19:** 2164–2175.

Zgurski, J.M., Sharma, R., Bolokoski, D.A., and Schultz, E.A. (2005). Asymmetric auxin response precedes asymmetric growth and differentiation of asymmetric leaf1 and asymmetric leaf2 *Arabidopsis* leaves. Plant Cell **17:** 77–91.

Zhou, C., Han, L., Hou, C., Metelli, A., Qi, L., Tadege, M., Mysore, K.S., and Wang, Z.Y. (2011a). Developmental analysis of a *Medicago truncatula* smooth leaf margin1 mutant reveals context-dependent effects on compound leaf development. Plant Cell **23:** 2106–2124.

Zhou, C., et al. (2011b). From model to crop: Functional analysis of a STAY-GREEN gene in the model legume *Medicago truncatula* and effective use of the gene for alfalfa improvement. Plant Physiol. **157:** 1483–1496.